

**DEVELOPMENT OF A METHOD TO INVESTIGATE INTRA-MOLECULAR
PROTON MIGRATION DURING COLLISION INDUCED DISSOCIATION
OF GAS-PHASE PEPTIDES**

A Thesis by

Qun Wu

M.S., Sichuan University, Sichuan, China, 1994

B.S., Sichuan University, Sichuan, China, 1991

Submitted to the College of Liberal Arts of Sciences
and the faculty of the Graduate School of
Wichita State University in partial fulfillment of
the requirements for the degree of
Master of Science

December 2005

**DEVELOPMENT OF A METHOD TO INVESTIGATE INTRA-MOLECULAR
PROTON MIGRATION DURING COLLISION INDUCED DISSOCIATION
OF GAS-PHASE PEPTIDES**

I have examined the copy of this thesis for form and content and recommend that it be accepted in partial fulfillment of the requirements for the degree of Master of Science, with a major in Chemistry.

Michael Van Stipdonk, Committee Chair

We have read this thesis
and recommend its acceptance:

Erach R. Talaty, Committee Member

Francis D'Souza, Committee Member

David M. Eichhorn, Committee Member

J. David McDonald, Committee Member

ACKNOWLEDGEMENTS

I would like to express my sincere thanks to my advisor, Dr. Michael Van Stipdonk for what he has done for me throughout my studies at Wichita State University. He is a great teacher, a great researcher and a great advisor. It is my honor to be his student.

I also would like to extend my appreciation to the members of my thesis committee, Dr. Talaty, Dr. D'Souza, Dr. Eichhorn and Dr. McDonald for kindly accepting to be my committee and giving me good advice on my thesis.

Furthermore, I need to express my devout thankfulness to all of my group members and colleagues and friends for their support.

Finally, I am deeply grateful to my family for their love and support. To my husband, Xiangdong Gan, my lovely son Xiaoke Gan and my parents Rongfu Wu, Xianxie Gu, thank you for your love and encouragement.

For the funding sources, I would like to acknowledge National Science Foundation (CAREER-0239800), Kansas NSF EPSCoR Program and Kansas Technology Enterprise Corporation, NIH K-BRIN Program and Lloyd Parker Fellowship.

ABSTRACT

Use of a combination of hydrogen/deuterium (H/D) exchange, mass spectrometry (MS) and/or CID is a rapidly evolving approach to the investigation of protein structure and conformation and the dynamics of conformational change. It has been noted, however, interpretation of CID MS data on partially deuterated peptide ions can, in principle, be hampered by both inter- and intramolecular migration of hydrogen and deuterium atoms. In this study, an isotope tracer was produced in situ by a McLafferty-type rearrangement of C-terminal peptide *tert*-butyl esters. This rearrangement generates a peptide with a C-terminal acid group with an isotope label. The label can then be traced through multiple CID stages to determine the amount of intra-molecular migration and scrambling of protons among exchangeable sites. Experimental results from a series of Li⁺ cationized sarcosine substitution peptides show that the C-terminal acid and amide positions, and the amide position adjacent to the C-terminus, allow the exchange of the isotope label. Transfer to the amide position at the N-terminus, the position for which the distance from the site at which the isotope tracer was initially generated is the greatest, appears to be less favored.

The influence of amino acids and cations on intramolecular proton migration was also investigated. Three series of peptides AcSarGXOtBu, AcGSarXOtBu, AcSarSarXOtBu (where X was glycine(G), alanine(A), valine(V), leucine(L), phenylalanine(F)) together with three cations Li⁺, Na⁺ and Ag⁺ were used in this study. The results show that amino acids and cations have only a slight effect on the amount of proton migration observed.

TABLE OF CONTENTS

CHAPTER	PAGE
1. INTRODUCTION.....	1
2. EXPERIMENTAL METHODS	7
2.1 Mass Spectrometry (MS) and Tandem Mass spectrometry (MS/MS).....	7
2.2 Electrospray Ionization (ESI).....	11
2.3 Quadrupole Ion Trap Analyzer.....	13
2.4 Reagents and experimental procedure.....	18
3. GENERATION OF ISOTOPE LABEL AT C-TERMINAL BY MC-LAFFERTY-TYPE REARRANGEMENT.....	21
3.1 Generation of Isotope Label at C-terminals by McLafferty-type rearrangement.....	21
3.2 Influence of two important CID Parameters.....	30
3.3 Summary.....	31
4. INFLUENCE OF POSITION AND NUMBER OF AMIDE EXCHANGEABLE SITES ON PEAK SPLITTING.....	33
4.1 Results from a Series of Sarcosine Substitution Peptides.....	33
4.2 Summary.....	38
5. INFLUENCE OF AMINO ACIDS AND CATIONS ON INTRAMOLECULAR PROTON MIGRATION FROM THREE SERIES OF TRI-PEPTIDES.....	39
5.1 Introduction.....	39
5.2 AcSarGXOtBu Series.....	40

5.3 AcGSarXOtBu Series.....	41
5.4 AcSarSarXOtBu Series.....	42
5.5 Summary.....	42
6. CONCLUSIONS AND FUTURE WORK.....	50
REFERENCES.....	54

LIST OF FIGURES

	PAGE
Figure 2.1 The principle of mass spectrometry and tandem mass spectrometry.....	9
Figure 2.2 Diagram shows the multiple stage tandem mass spectrometry.....	10
Figure 2.3 Biemann nomenclature and spectra of the fragment ions produced from the protonated and Li cationized valine-alanine-alanine-phenylalanine (VAAF) tetra peptide.....	12
Figure 2.4 Schematic diagram of of an electrospray ion source.....	14
Figure 2.5 Schematic of a quadrupole ion trap.....	15
Figure 2.6 Typical stability diagram for a quadrupole ion trap.....	17
Figure 3.1 Three mass spectra generated from $[\text{AcGGG-OtBu+Li}]^+$ (a) Isolation of $[\text{AcGGG-OtBu+Li}]^+$ at m/z 294. (b) CID of $[\text{AcGGG-OtBu+Li}]^+$. (c) CID (MS^3) of $[\text{AcGGG-OH+Li}]^+$ generated from $[\text{AcGGG-OtBu+Li}]^+$	22
Figure 3.2 Four major product ions of $[\text{AcGGG-OH+Li}]^+$ (a) $(b_2+17+Li)^+$ (b) $(b_2-1+Li)^+$ (c) $(a_2-1+Li)^+$ (d) $(M-H_2O+Li)^+$	23
Figure 3.3 Three mass spectra generated by CID of three forms of AcGGG (a) CID of $[\text{AcGGG-OH+Li}]^+$. (b) CID of $[(d_3)\text{AcGGG-OH+Li}]^+$ formed from $(d_3)\text{AcGGG-OtBu+Li}^+$ by McLafferty rearrangement. (c) CID of $[(d_3)\text{AcGGG-OD+Li}]^+$ (the numbers in the parenthesis represent mass shifts)	27
Figure 3.4 CID of Li+ cationized $(d_3)\text{AcGGG-OH}$ generated from $(d_3)\text{AcGGG-OtBu}$	32
Figure 4.1 Precursor species, potential intermediates to $[b_2+17+cat]^+$ of peptides AcGGG, AcSarGG, AcGSarG, AcGGSar, AcSarSarG.....	34
Figure 4.2 CID of $[(d_3)\text{AcGGG-OH+Li}]^+$, $[(d_2)\text{AcGGSar-OH+Li}]^+$, $[(d_2)\text{AcGSarG-OH+Li}]^+$, $[(d_2)\text{AcSarGG-OH+Li}]^+$,	

	[[<i>d</i>]AcSarSarG-OH+Li] ⁺ . In each case, species fragmented were derived by McLafferty rearrangement from <i>t</i> -butyl esters to generate isotope tracer.....	37
Figure 5.1	Precursor species, potential intermediates to [b ₂ +17+cat] ⁺ of peptides AcSarGX (X=G, A, V, L, F).....	44
Figure 5.2	Elimination of D versus the elimination of H as part of the neutral imine product in forming [b ₂ +17+cat] ⁺ of peptides AcSarGX (X=G, A, V, L, F) with different cations. (a) Li ⁺ (b) Na ⁺ (c) Ag ⁺ (the error bars represents the standard deviation based on three trials).....	45
Figure 5.3	Precursor species, potential intermediates to [b ₂ +17+cat] ⁺ of peptides AcGSarX (X=G, A, V, L, F).....	46
Figure 5.4	Elimination of D versus the elimination of H as part of the neutral imine product in forming [b ₂ +17+cat] ⁺ of peptides AcGSarX (X=G, A, V, L, F) with different cations. (a) Li ⁺ (b) Na ⁺ (c) Ag ⁺ (the error bars represents the standard deviation based on three trials).....	47
Figure 5.5	Precursor species, potential intermediates to [b ₂ +17+cat] ⁺ of peptides AcSarSarX (X=G, A, V, L, F).....	48
Figure 5.6	Elimination of D versus the elimination of H as part of the neutral imine product in forming [b ₂ +17+cat] ⁺ of peptides AcSarSarX (X=G, A, V, L, F) with different cations. (a) Li ⁺ (b) Na ⁺ (c) Ag ⁺ (the error bars represents the standard deviation based on three trials).....	49

LIST OF SCHEMES

	PAGE
Scheme 1 Generation of isotope tracer by McLafferty-type rearrangement.....	5
Scheme 2 Formation of $(b_2+17+Li)^+$ from $[AcGGG-OH+Li]^+$	25
Scheme 3 Formation of $(b_2-1+Li)^+$ from $[AcGGG-OH+Li]^+$	26

CHAPTER 1

INTRODUCTION

The conformation of a protein, determined in part by amino acid sequence, is important to the function of the biomolecules in solution. It was recognized nearly 50 years ago that different protein structures undergo isotope exchange at different rates, and this has led to widespread use of hydrogen-deuterium exchange (HDX) as a means to study protein conformation using nuclear magnetic resonance (NMR) spectroscopy monitored, and more recently mass spectrometry (MS) [1-3].

In solution, HDX can be used to obtain information about the solvent accessibility of amino acid residues in a protein. Sites of exchange can be localized to the individual amino acid by using NMR or to larger portions of the protein by using proteolytic enzymes (typically pepsin) and mass spectrometric analysis of the products. From these experiments, information about the tertiary structure of proteins in solution can be deduced [4]. Mass spectrometric methods, when used for probing protein conformations by HDX, offer certain advantages in comparison to NMR methods. These advantages include the ability to (a) study proteins in the micromolar as opposed to the millimolar range, (b) study proteins that precipitate or aggregate at high concentrations or that are larger than 20kDa, (c) observe coexisting conformations simultaneously, (d) work with mixtures or nonpurified samples, and (e) determine the exact hydrogen isotope content [2, 5]. The most compelling reason for the use of MS over NMR

for measuring HDX is that larger proteins and lower amounts of samples can be studied. In addition mass spectrometry can provide structural details on transient or folding intermediates that may not be accessible by CD, fluorescence and NMR because these techniques measure the average properties of large populations of proteins in solution [6].

H/D exchange has also been used to infer peptide conformations in the gas phase and determine the number of active hydrogens. The application of mass spectrometry (MS) to monitor HDX in peptides and proteins was first introduced by Katta and Chait in 1991 [7]. With the emergence of the so-called “soft” ionization techniques, gas-phase HDX in combination with electrospray ionization mass spectrometry (ESI-MS) and/or tandem MS has become a useful tool to study protein structure and conformation [8-14].

Briefly, the conventional mass spectrometry approach involves the exchange of protons at amide, amino and acid positions for deuterium by incubation in deuterated solvent, followed by enzymatic cleavage, ionization and characterization by MS with or without collision induced dissociation (CID). It is assumed that those amide positions along a protein that are exposed to solvent will undergo HDX, while those inhabiting the interior or core regions of a folded protein will either not exchange or will exchange at a significantly lower rate. Enzymatic cleavage and analysis by MS then reveals the extent to which various stretches of amino acid sequence have exchanged H for D, and thus provide details about protein conformation in solution. It is believed that intermolecular exchange can also take place when peptide ions in the gas phase undergo

collisions with gaseous H₂O or D₂O in the relatively high-pressure region at the interface. Such bimolecular H/D exchange reactions of peptides and proteins in the gas phase have been studied extensively [7, 13-16], and exchange rates have been proposed to be dependent on a number of factors, including gas-phase proton affinity, accessibility of exchangeable sites at the surface, and the structure of the molecules.

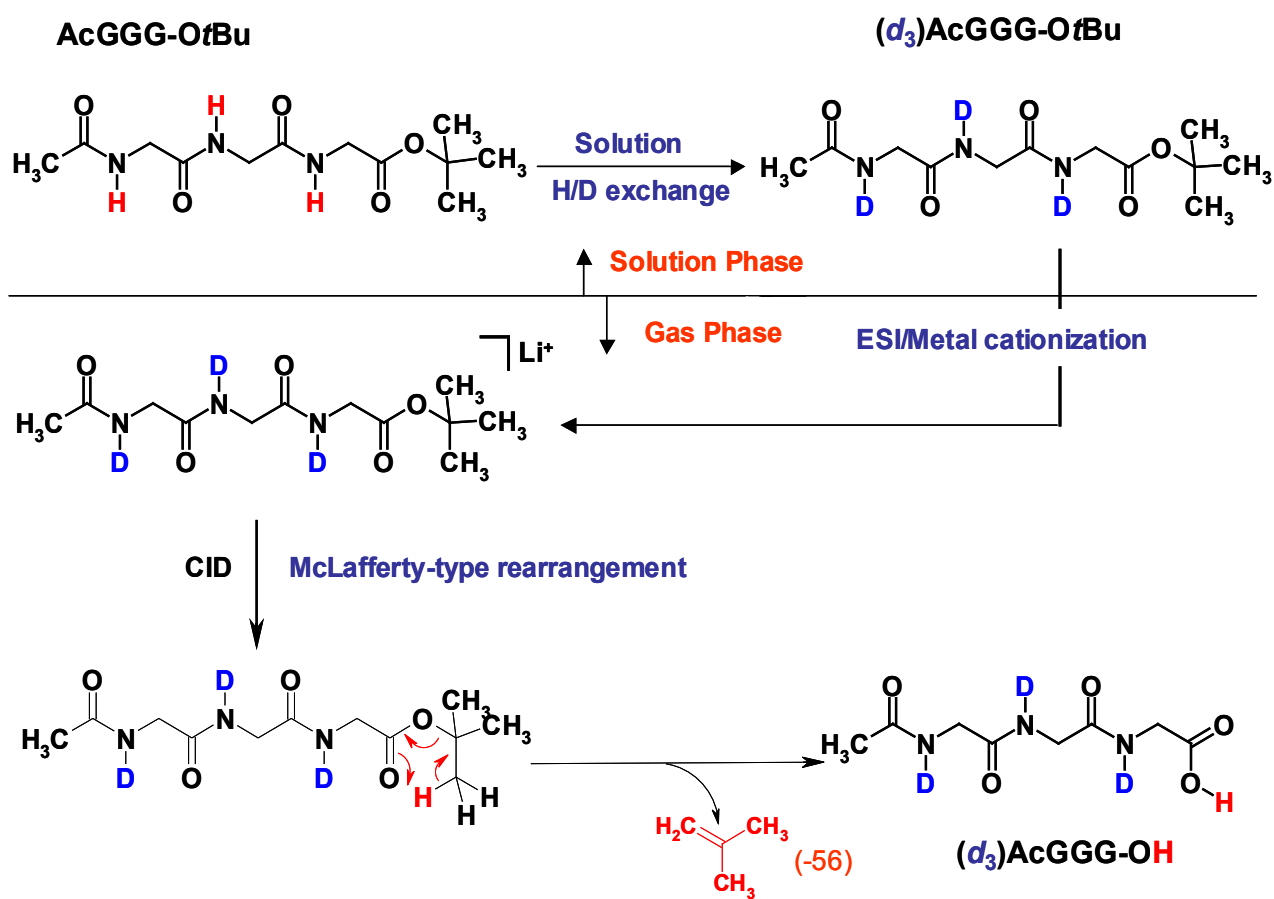
It has been noted, however, interpretation of CID MS data on partially deuterated peptide ions can, in principle, be hampered by both inter- and intramolecular migration of hydrogen and deuterium atoms [10]. In the literature, the degree to which “proton scrambling” influences the accuracy of the HDX CID experiment has been debated. In several studies, it has been shown that hydrogen mobility within peptide ions is sufficiently rapid to scramble their position even prior to collisional activation [14, 17, 18], whereas in other studies, it has been claimed that intramolecular migration of amide hydrogens is minor or even negligible [5, 6, 8, 9, 11]. As H/D exchange in combination with CID MS is used more and more for structural and conformational investigations of proteins and peptides, it is very important to understand the factors underlying deuterium scrambling and to find ways to control or prevent this process.

The work in this project involved the development and optimization of a novel method that may be of utility in the investigation of the extent to which intramolecular proton migration may occur in CID/MS experiments and the influence of factors such as cation choice and sequence on the amount of scrambling observed. The approach is based upon the recent report that metal

cationized peptides containing C-terminal ethyl, isopropyl or *tert*-butyl ester groups will undergo facile McLafferty-type rearrangement. The rearrangement results in the generation of a metal cationized peptide with a C-terminal acid group [19]. The working hypothesis in these studies was the following: CID of peptide-esters, incubated in deuterated solvent prior to the MS experiment, should generate by McLafferty-type rearrangement a peptide with amide position deuterium atoms, and a C-terminal –OH group. This, in effect, would be the in-situ generation of an isotope tracer, a site-specific isotope label that can then be traced through multiple CID stages, and thus probe intra-molecular proton migration (Scheme 1). A similar tracer might be generated at the N-terminus of a peptide by using a *t*-butoxycarbonyl (Boc) protecting group.

The first objective of this research was to determine whether CID of deuterium labeled peptide, *tert*-butyl esters will generate an isotope label at the C-terminus by McLafferty-type rearrangement, and whether isotope scrambling can/will be detected during CID by observing splitting of product ions into isotopic peaks.

The second objective was to investigate the influence of position and number of amide exchangeable sites on the peak splitting by using a series of acetylated tripeptides esters with site-specific incorporation of sarcosine, an amino acid that features an N-methyl group (i.e. no amide HDX is possible). To carry out these two objectives, five acetylated tripeptide esters AcGGGOTBu, AcSarGGOTBu, AcGSarGOTBu, AcGGSarOTBu, AcSarSarGOTBu and cation Li^+ were used.



Scheme 1. Generation of isotope tracer by McLafferty-type rearrangement

The third objective of was to determine whether the amount of isotope scrambling is influenced by the specific position of amino acids such as glycine(G), alanine(A), valine(V), leucine(L), phenylalanine(F), or on the choice of metal cation. The extent of intramolecular proton migration was measured by monitoring the splitting of the $(b_2+17+Cat)^+$ product ion once the isotope label was generated in-situ via McLafferty-type rearrangement. This product ion was chosen because its formation mechanism (see chapter 3, scheme 2) directly involved the transfer of the isotope label [20]. Three series of synthetic acetylated tripeptide esters AcSarGXOtBu, AcGSarXOtBu, AcSarSarXOtBu (where X= G, A, V, L, F) together with 3 different cations Li^+ , Na^+ , Ag^+ were used in the study.

CHAPTER 2

EXPERIMENTAL METHODS

2.1 Mass Spectrometry (MS) and Tandem Mass spectrometry (MS/MS)

Mass spectrometry is a powerful analytical technique that is used to identify unknown compounds, to quantify known compounds, and to elucidate the structure and chemical properties of molecules according to their mass to charge ratio (m/z). Tandem mass spectrometry, abbreviated as MS/MS, employs at least two stages of mass analysis to examine selectively the fragmentation of an ion of interest and to determine/confirm composition and structure through close examination of fragment ions produced by and neutrals eliminated in gas-phase dissociation reactions. In general, ions of a particular m/z value are selected in the first stage of mass analysis. These precursor ions are accelerated by means of applied electric fields to increase their kinetic energy. Energetic collisions between the accelerated ions and a background gas such as He raise the internal energies of the former and induce unimolecular dissociation reactions. The masses of the product ions are then determined using a second stage of mass analysis. Pioneering efforts in the area of MS/MS include the work of Beynon, Cooks and co-workers on reverse geometry magnet instruments, the development of collision-activated or collision-induced dissociation (CID) by McLafferty *et al.* and Jennings and the introduction of the triple quadrupole mass spectrometer by Yost and Enke [21-25].

Basically, a tandem mass spectrometer can be conceived in two ways: in space by the coupling of two physically distinct instruments or in time by performing an appropriate sequence of events in an ion storage device. Thus they are two main categories of instruments that allow MS/MS experiments: tandem mass spectrometers in space or in time.

Common tandem-in-space instruments have at least two mass analyzers and each mass analyzer performs separately to accomplish the different stages of the analysis. The tandem quadrupole mass spectrometer is an example for a tandem-in-space mass spectrometer. Two analyzers are assembled in tandem. The first analyzer is used to isolate a precursor ion, which then undergoes spontaneously or by some activation reactions to yield product ions and neutral fragments in a collision cell which is placed between the two mass analyzers. The product ions are then analyzed in the second analyzer. The principle is illustrated in figure 2.1.

The second category tandem-in time instruments comprise one analyzer which is capable of storing ions. An ion trap mass spectrometer is an example for such a system, in which one analyzer is used multiple times. These devices allow the selection of particular ions by ejection of all others. The selected ion can be excited and caused to fragment during a selected time period, and the fragment ions can be observed in a mass spectrum.

To get more information about the fragmentation pathways of ions, and molecular composition and structure, multiple stages of tandem mass spectrometry can be used. These experiments are defined as MS^n , where n

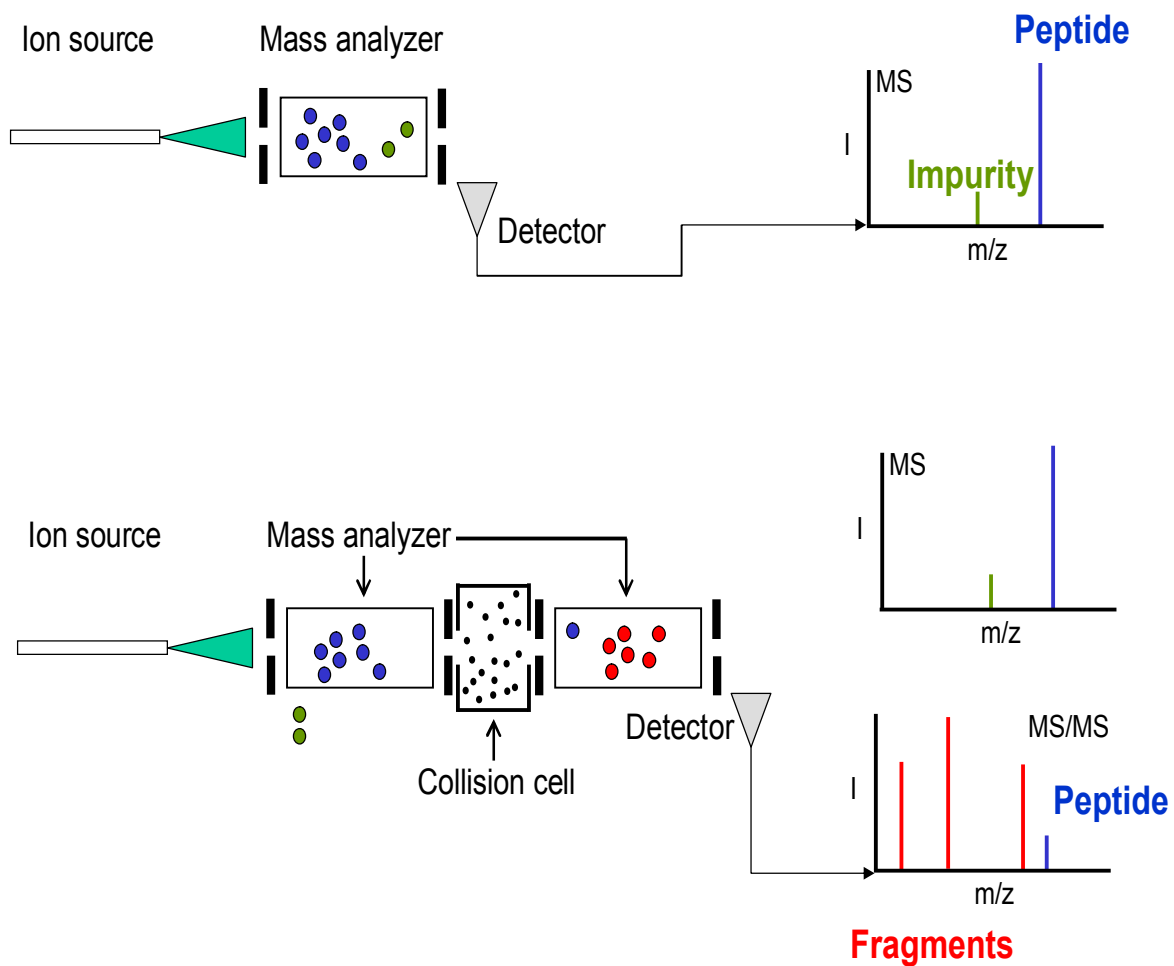


Figure 2.1 The principle of mass spectrometry and tandem mass spectrometry.

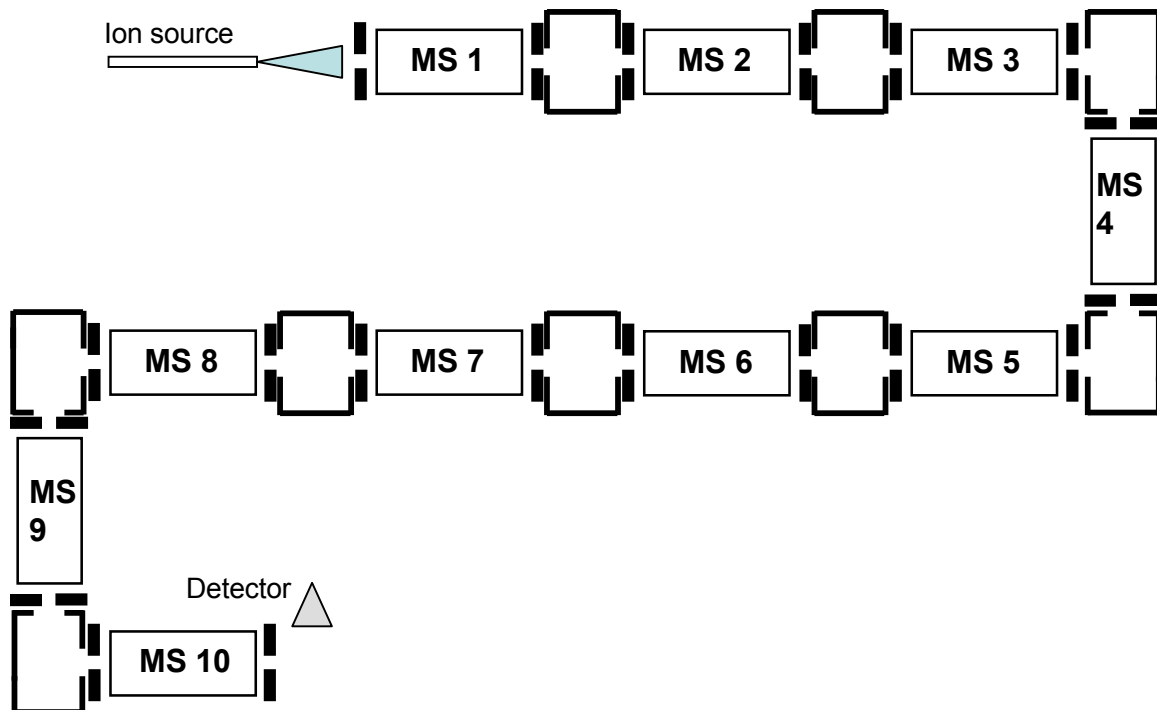


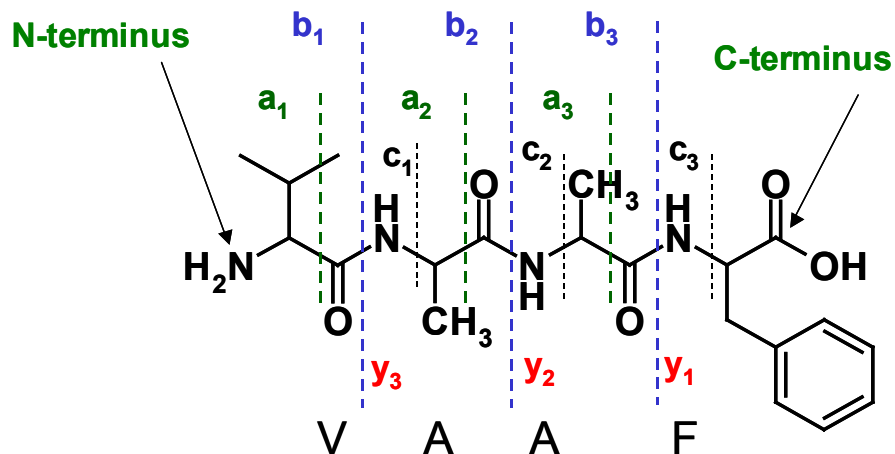
Figure 2.2 Diagram shows the multiple stage tandem mass spectrometry

refers to the number of generations of ions being analyzed. In figure 2.2 a precursor ion is selected by the first spectrometer (MS1), fragmented through a collision cell and the fragments are analyzed by the second spectrometer (MS2). Then the fragment ions can go through another collision cell, get fragmented and analyzed by the third spectrometer (MS3). This process may be repeated up to 10 times as shown. While impractical for tandem-in-space configurations, the multiple-stage experiments are possible using the tandem-in-time nature of ion trapping instruments like the quadrupole ion trap.

In these studies, a Finnigan LCQ-DecaTM ion ion-trap mass spectrometer (Thermoquest Corporation; San Jose, CA, USA) was used. Figure 2.3 gives an example of the tandem mass spectra generated from protonated and Li cationized VAAF (valine-alanine-alanine-phenylalanine). Here the nomenclature proposed by Roepstorff and Fohlman, and later modified by Biemann has been used. The product ions formed include b_n type ions (by dissociating through amide bond), a_n type ions (which remove another carbonyl) and c_n type ions (involving cleavage between the amine and R group) and all contain the N-terminus of the original peptide. The y_n type (from cleavage of the amide bond) and z_n type ions (from cleavage between amine and R group) instead contain the C-terminus. The mass difference between the parent ion and the resulting product ions of a given product ion series (e.g. b ions) correspond to the masses of the residues eliminated from the peptide during the fragmentation reactions, and often allow the sequence of the peptide to be determined. Because x_n , z_n and c_n type ions are not common under the experimental conditions encountered in the quadrupole ion trap, this study was focused on b_n type ions.

2.2 Electrospray Ionization (ESI)

Electrospray ionization (ESI) is a soft ionization technique that accomplishes the transfer of ions from solution to the gas phase. The first experiments with the technique were carried out by Chapman in the late 1930s [26], and later advanced into a practical ionization method for mass spectrometry by Dole et al. [27,28]. Fenn, Mann and coworkers were responsible for the



VAAF

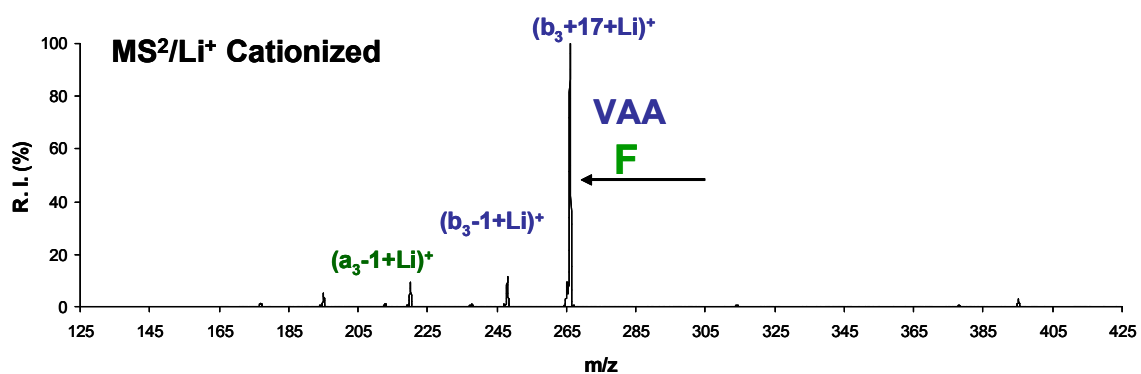
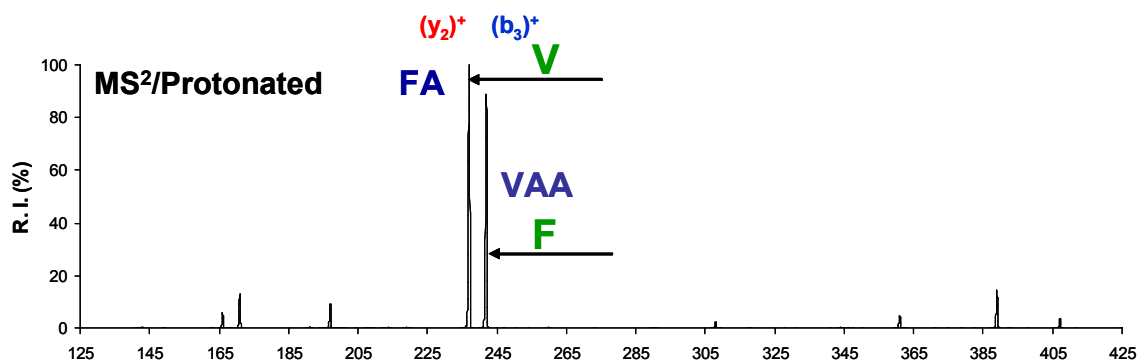


Figure 2.3 Biemann nomenclature and spectra of the fragment ions produced from the protonated and Li cationized valine-alanine-alanine-phenylalanine (VAAF) tetra peptide

development of the modern-day technique of electrospray ionization mass spectrometry (ESI-MS) [29, 30].

In the ESI source (figure 2.4), a dilute sample solution (typically 10^{-4} - 10^{-6} M) is pumped through a narrow-bore needle at μl per minute rates. A potential of ca. 3-4 kilovolts, relative to a counter electrode, is applied to the needle. The applied field causes the accumulation of charge on the surface of the liquid as it exits the needle, causing the solution to break-up into small, highly charged droplets. The resulting aerosol thus generated encounters a stream of nitrogen gas that assists the evaporation of solvent from the droplets. Transit of the droplets through a heated metal capillary continues the desolvation process, causing the droplet size to decrease until the Rayleigh limit is reached. At this point, Coulombic repulsion due to the high charge state overcomes the droplet's surface tension and the droplet explodes. The 'Coulombic explosion' creates smaller, lower charge-state droplets, which continue to desolvate until individually charged, essentially bare analyte ions are formed. The ions are then transferred through lenses and stages of differential pumping to the high vacuum environment of the mass spectrometer.

2.3 Quadrupole Ion Trap Analyzer

The quadrupole ion trap analyzer was invented by Paul and Steinwedel in 1960 [31] and was modified to a useful mass spectrometer by Stafford et al. of the Finnigan company in 1984 [32]. The quadrupole ion trap serves both as a device to confine gas-phase ions, and as a mass spectrometer with considerable

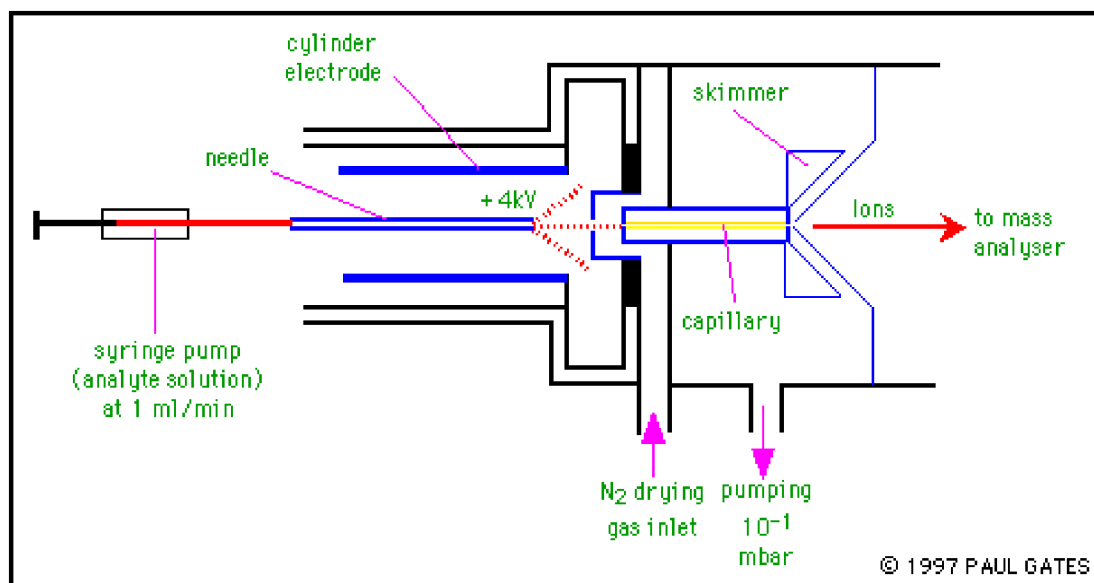


Figure 2.4 Schematic diagram of of an electrospray ion source

(© Paul Gates July 30th. 1997.

<http://www-methods.ch.cam.ac.uk/meth/ms/theory/esi.html>)

mass range and variable mass resolution. All of this is done at a pressure of 1 mtorr of helium buffer gas. The typical ion-trap mass analyzer is composed of a ring electrode with two endcap electrodes on the top and the bottom (figure 2.5).

The confining capacity of the “electric field test-tube” arises from the formation of a trapping potential well when appropriate potentials are applied to the electrodes of the ion trap. The confinement of gaseous ions permits the study of gas-phase ion chemistry and the elucidation of ion structures by use of repeated stages of mass selection known as tandem-in-time mass spectrometry.

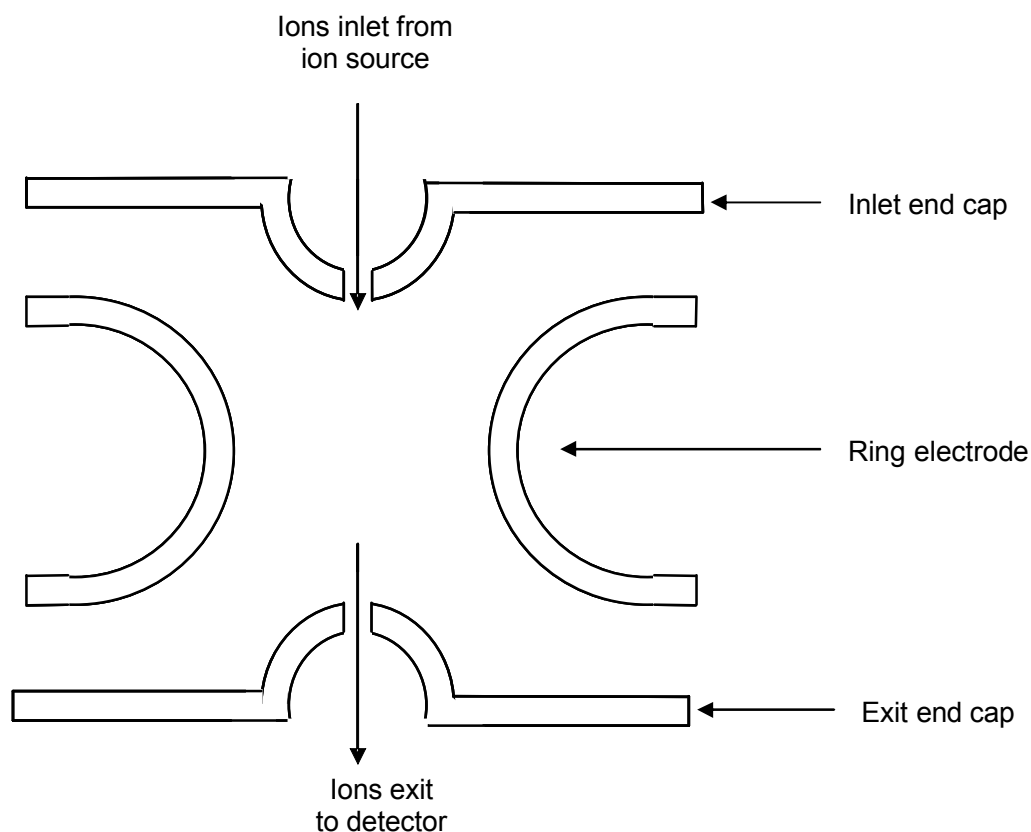


Figure 2.5 Schematic of a quadrupole ion trap

In addition, the ion trap can be used as a mass spectrometer by sequentially scanning out ions of a given mass/charge ratio into a detector. Ions created by electrospray ionization are gated into the ion trap using an electrostatic lensing system. The ion trap is typically filled with helium to a pressure of about 1 mtorr. Collisions with helium dampen the kinetic energy of the ions and serve to quickly contract trajectories toward the center of the ion trap, enabling trapping of injected ions. Trapped ions are further focused toward the center of the trap through the use of an oscillating potential, called the

“fundamental rf”, applied to the ring electrode. Ions will adopt stable trajectories and be trapped depending upon the values for the mass and charge of the ion, the size of the ion trap (r), the oscillating frequency of the fundamental rf (ω), and the amplitude of the voltage on the ring electrode (V). The dependence of ion motion on these parameters is described by the dimensionless parameter q_z :

$$q_z = 4eV/mr^2\omega^2$$

An analogous parameter a_z describes the effect on the motion of ions when a DC potential is applied to the ring electrode.

To create an ideal quadrupole field, $r^2=2z^2$ is required, where z is the axial distance from the center of the trap to the endcap electrode. A “stability diagram” (figure 2.6) shows a theoretical region where radial and axial stability overlap. Depending upon the amplitude of the voltage placed on the ring electrode, an ion of a given m/z will have a_z , q_z values that will fall within the boundaries of the stability diagram, and the ion will be trapped. If the a_z , q_z values at that voltage falls outside of the boundaries of the stability diagram, the ion will hit the electrodes and be lost.

Trapped ions oscillate in the trap with a frequency known as the secular frequency that is determined by the values for a_z , q_z and the frequency of the fundamental rf. Resonance conditions are induced by applying an ac voltage to the endcap electrodes and the q_z value of an ion of interest is changed until the secular frequency of the ion matches the frequency of the applied ac voltage. Individual ions are isolated by the application of a waveform signal across the

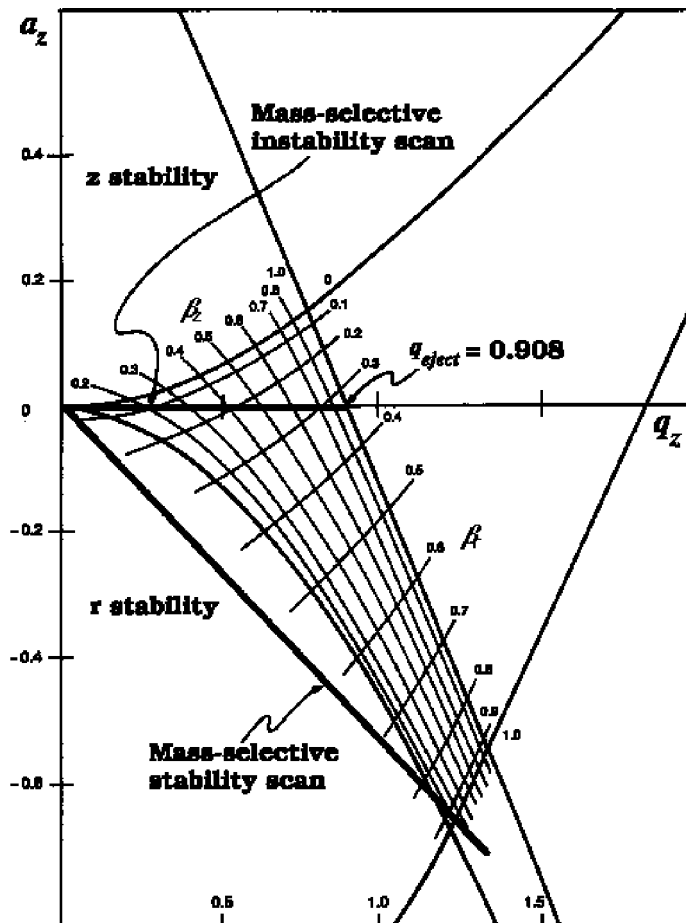


Figure 2.6 Typical stability diagram for a quadrupole ion trap.

endcap electrodes. Collisional activation in the ion trap is accomplished by applying low-amplitude voltages at resonance values for individual ions to the endcap electrodes. The ion motion between the endcaps increases, leading to ion dissociation due to thousands of collisions with the helium gas. This process causes random fragmentation along the peptide backbone. For detection of the ions, the potentials are altered to destabilize the ion motions resulting in ejection

of the ions through the exit endcap. The ions are usually ejected in order of increasing m/z by a gradual change in the potentials. This 'stream' of ions is focussed onto the detector of the instrument to produce the mass spectrum.

2.4 Reagents and experimental procedure

Glycine-Glycine(GG), Glycine-Sarcosine(GSar), Sarcosine-Glycine (SarG), Sarcosine-Sarcosine(SarSar), Sarcosine(Sar); Glycine *tert*-butyl ester, Sarcosine *tert*-butyl ester, Alanine *tert*-butyl ester, Valine *tert*-butyl ester, Leucine *tert*-butyl ester, Phenylalanine *tert*-butyl ester, acetic anhydride, acetic acid, D₂O, CH₃OD, LiNO₃, NaNO₃, AgNO₃ and were purchased from Sigma-Aldrich (St. Louis, MO). CH₂Cl₂, CH₃OH were purchased from Fisher (Pittsburgh, PA). Polymer resin bound carbodiimide were purchased from Argonaut (Foster City, CA) and used as received.

To prepare acetylated versions of the peptides used in this study, the dipeptides, such as GG, GSar, SarG, SarSar were dissolved in acetic anhydride and acetic acid (1:5 by volume) and incubated in sand bath at 38°C for 3 hours and evaporated to get rid of the excess acetic anhydride and acetic acid. The acetylated peptides (1.5 equiv) in CH₂Cl₂ were then added to the dry PS-Carbodiimide resin (2.0 equiv) and the mixture stirred at room temperature. After 15 minutes, the *tert*-butyl esters (1.0 equiv) in CH₂Cl₂ were added and this coupling reaction was carried out at room temperature for a minimum of 8 hours, after which the resin was filtered and the remaining solution was evaporated to

dryness. The acetylated peptide *tert*-butyl esters were used without further purification.

Solutions of each acetylated peptide ester were prepared by dissolving the appropriate amount of solid material in a mixture (1:1 by volume) of CH₃OH and H₂O or CH₃OD and D₂O to produce final concentrations of 10⁻⁵-10⁻⁴M. Equimolar metal nitrate solutions were prepared in H₂O and D₂O. Electrospray ionization (ESI) mass spectra were collected using a Finnigan LCQ-Deca™ ion-trap mass spectrometer (ThermoFinnigan; San Jose, CA). Mixtures (1:1 by volume) of metal nitrate and peptide, prepared by mixing 0.25 mL of the respective stock solutions, were infused into the ESI-MS instrument using the incorporated syringe pump at a flow rate of 3-5 µL/min. The atmospheric pressure ionization stack settings for the LCQ (lens voltages, quadrupole and octapole voltage offsets, etc.) were optimized for maximum (M+Cat)⁺ ion transmission to the ion trap mass analyzer by using the auto-tune routine within the LCQ Tune program. Following the instrument tune, the spray needle voltage was maintained at +5 kV, the N₂ sheath gas flow at 25 units (arbitrary for the LCQ system, corresponding to approximately 0.375 L/min) and the capillary (desolvation) temperature at 200° C. The ion trap analyzer was operated at a pressure of ~1.5 x 10⁻⁵ Torr. Helium gas, admitted directly into the ion trap, was used as the bath/buffer gas to improve trapping efficiency and as the collision gas for CID experiments.

The multi-stage studies were performed as follows. The protonated, deuterated and metal cationized peptides were isolated for the initial CID stage (MS/MS) using an isolation width of 1.0-1.5 mass to charge (m/z) units. The

argentinated (M+Ag)⁺ peptides were isolated using a width of 6 m/z units, with the isolation mass centered between the ¹⁰⁷Ag and ¹⁰⁹Ag isotopic peaks. To induce collisional activation, the activation amplitude (which defines the amplitude of the R.F. energy applied to the end cap electrodes) for CID was set between 30 and 35% (chosen empirically) of 5 volts. The activation Q setting (as labeled by Thermoquest, is used to adjust the q parameter for the precursor ion during the CID experiment) was 0.30. The activation time employed at each CID stage was 30 msec.

CHAPTER 3

GENERATION OF ISOTOPE LABEL AT C-TERMINAL BY MC-LAFFERTY-TYPE REARRANGEMENT

3.1 Generation of Isotope Label at C-terminals by McLafferty-type rearrangement

The first objective of this research was to determine whether CID of the *tert*-butyl esters of deuterium labeled peptides would generate an isotope label at the C-terminus by McLafferty-type rearrangement, and whether the isotope scrambling could be detected during CID by observing “splitting” of product ions into isotopic peaks.

A previous study by Anbalagan *et al.* demonstrated that a McLafferty-type rearrangement could be used to generate metal cationized peptides with a C-terminal acid group from precursor peptides containing C-terminal *tert*-butyl ester groups [19]. Figure 3.1 shows three mass spectra generated from the Li⁺ cationized form of the C-terminal *tert*-butyl ester of acetylated glycine-glycine-glycine (AcGGG⁺OtBu). Figure 3.1 (a) shows the spectrum produced when Li⁺ cationized AcGGG⁺OtBu was isolated in the gas-phase environment of the ion trap without collisional activation. This was accomplished by isolating the ion from CID, but using a setting of 0% for the activation amplitude. Figure 3.1 (b) shows the result of subjecting ion to a single CID (MS/MS or MS²) stage using a setting of 30% for the activation amplitude. The only product ion generated after this stage was the Li⁺ cationized free-acid form of the peptide, AcGGG-OH at m/z

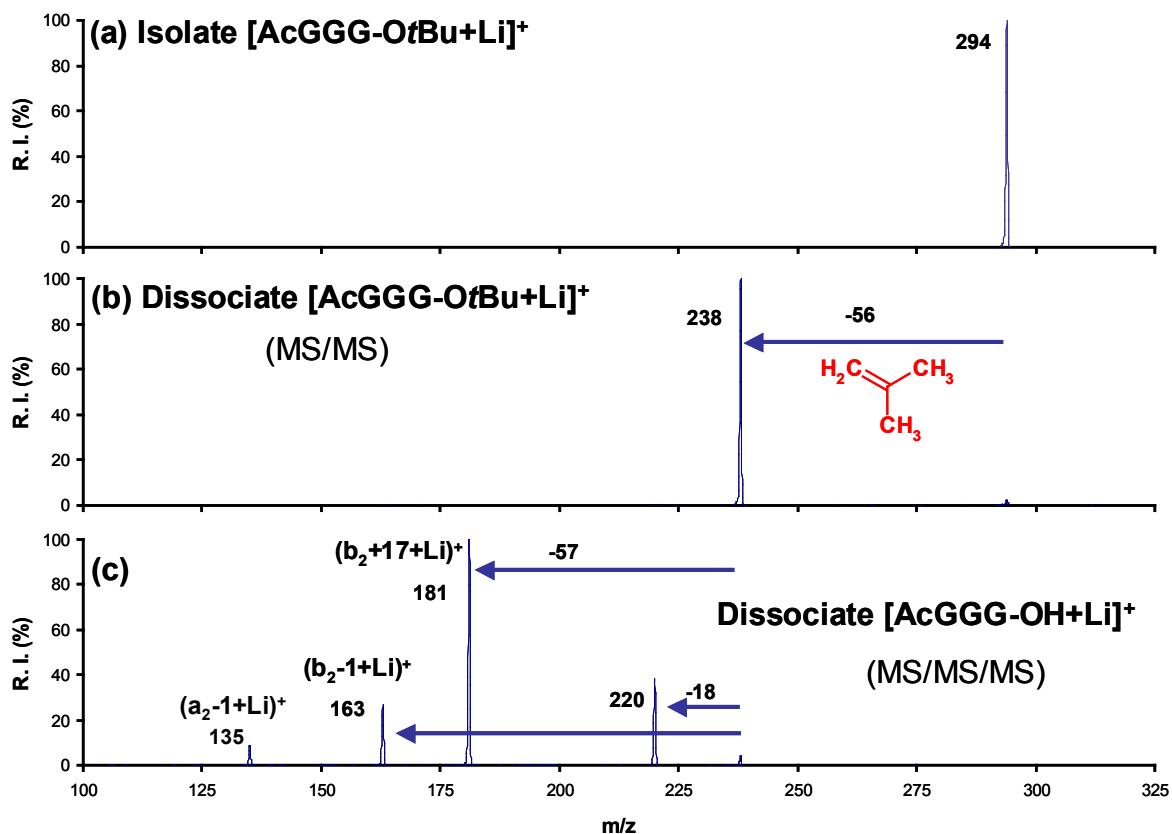
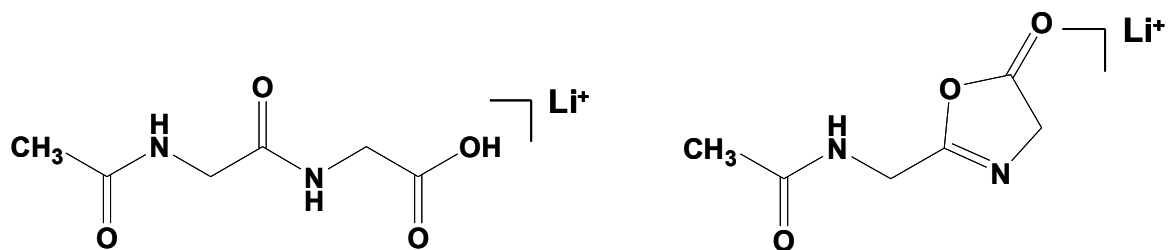


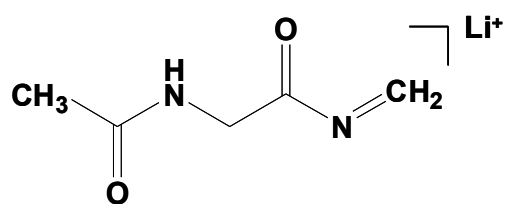
Figure 3.1 Three mass spectra generated from [AcGGG-OtBu+Li]⁺ (a) Isolation of [AcGGG-OtBu+Li]⁺ at m/z 294. (b) CID of [AcGGG-OtBu+Li]⁺. (c) CID (MS³) of [AcGGG-OH+Li]⁺ generated from [AcGGG-OtBu+Li]⁺

238, formed by the McLafferty-type rearrangement and the elimination of isobutene (a neutral loss of 56 Da (Dalton, defined as follows: 1 Da = (1/12) of the mass of a single atom of the isotope of carbon-12)). As shown in figure 3.1 (c), subsequent CID of Li⁺ cationized AcGGG-OH (MS/MS/MS or MS³) caused formation of several product ions, all characteristic of the fragmentation of AcGGG. The major peaks formed were: (M-H₂O+Li)⁺ at m/z 220 and the (b₂+17+Li)⁺, (b₂-1+Li)⁺ and (a₂-1+Li)⁺ sequence ions at m/z 181, 163, and 135 respectively. Figure 3.2 shows the structure of these four ions. In general, the

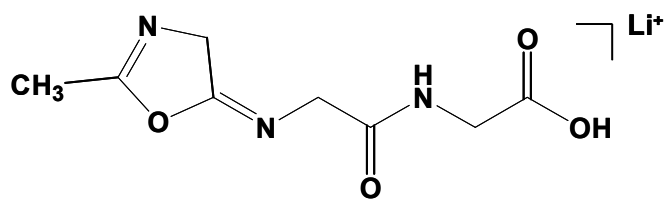


(a) $(b_2+17+Li)^+$

(b) $(b_2-1+Li)^+$



(c) $(a_2-1+Li)^+$

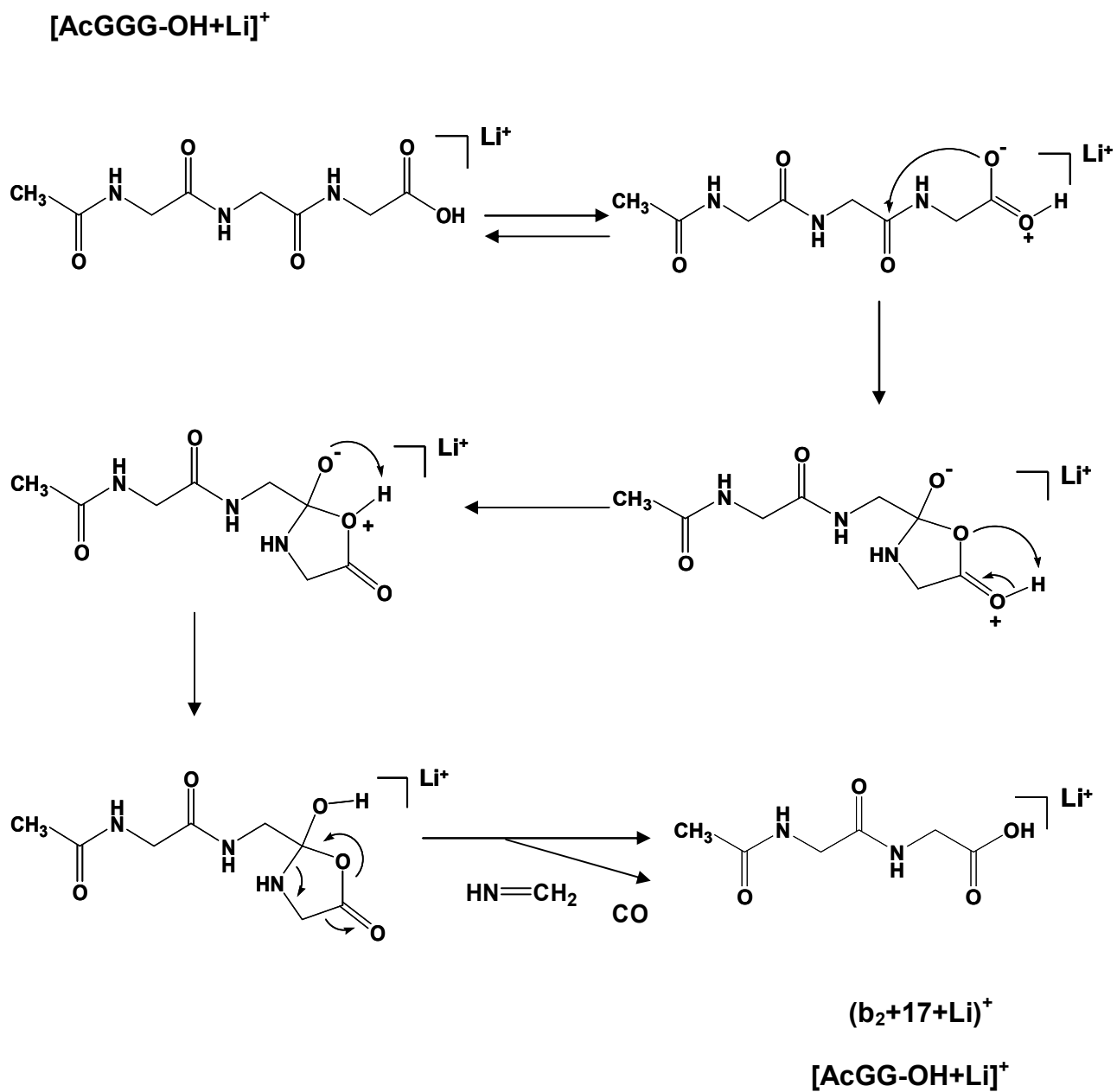


(d) $(M-H_2O+Li)^+$

Figure 3.2 Four major product ions of $[AcGGG-OH+Li]^+$ (a) $(b_2+17+Li)^+$ (b) $(b_2-1+Li)^+$ (c) $(a_2-1+Li)^+$ (d) $(M-H_2O+Li)^+$

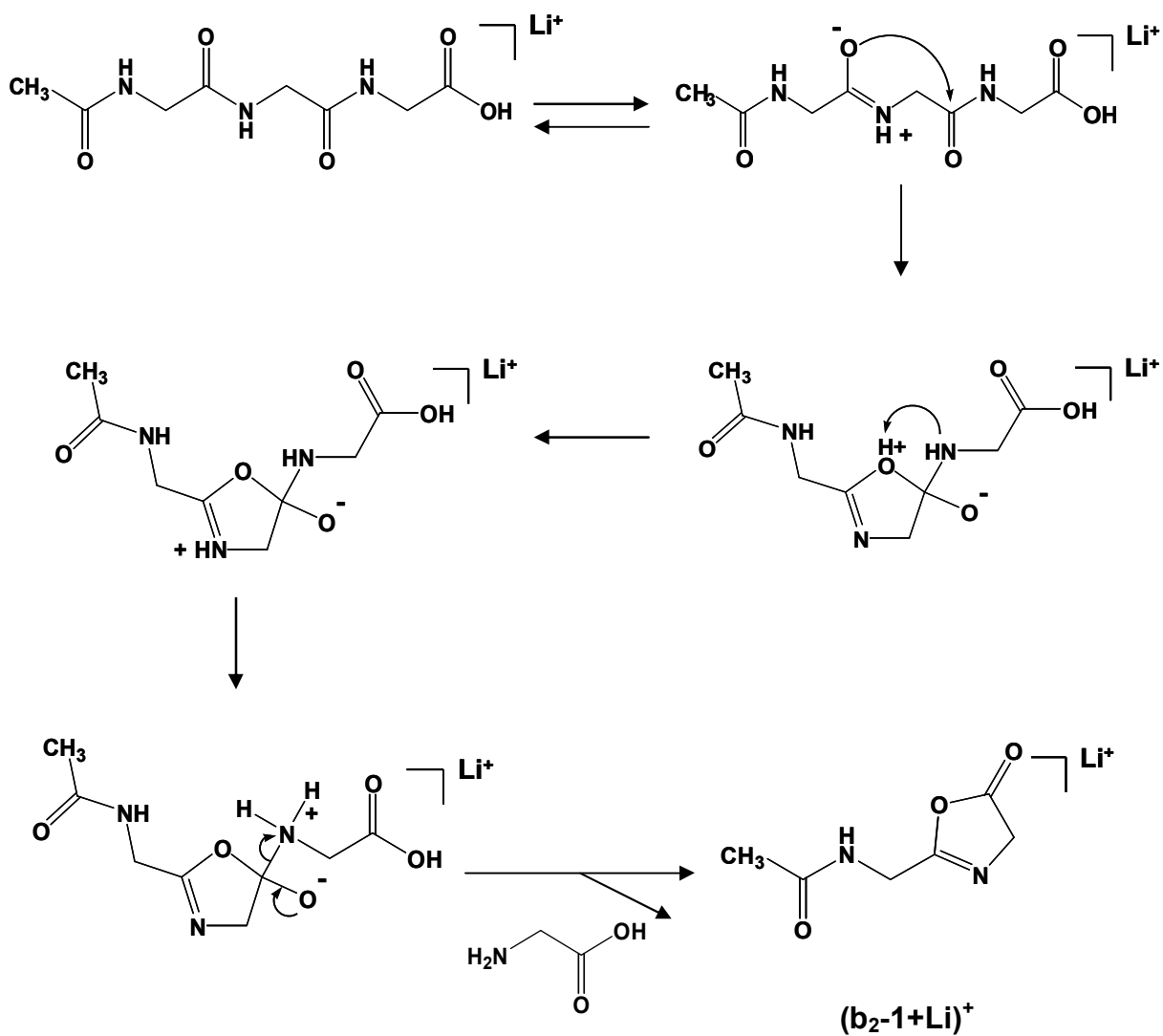
intensities of the $(b_2+17+Li)^+$ and $(b_2-1+Li)^+$ products observed in CID spectra reflect competition between two distinct unimolecular dissociation reactions. The formation of the $(b_2+17+Li)^+$ product ion (scheme 2) involves a nucleophilic attack on the carbonyl carbon of the amide bond being cleaved, by the oxygen atom of the C-terminal acid group [20, 33-36]. The formation of the $(b_2-1+Li)^+$ product ion (scheme 3) instead involves a nucleophilic attack on the carbonyl carbon at the cleavage site by an oxygen atom on the adjacent amide carbonyl group to the N-terminal side of the cleavage site [37, 38]. In both cases, formation of 5-membered rings is proposed to mediate the fragmentation reaction [39]. For this study, our focus was on the $(b_2+17+Li)^+$ species, because the formation mechanism for this ion directly involves the migration of the C-terminal -OH proton, that is, the one potentially generated as an isotope tracer in the McLafferty-type rearrangement.

Figure 3.3 shows three mass spectra generated by CID of three forms of AcGGG. In figure 3.3 (a), the spectrum was derived from Li^+ cationized AcGGG without a C-terminal ester group or amide position D atoms. Each product ion was observed as a single isotopic peak. Figure 3.3 (b) shows the spectrum resulting from the CID (MS^3) of $[(d_3)AcGGG-OH+Li]^+$ (the subscript here indicates the number of *amide*-position D atoms) that was initially created from CID (MS/MS) of $[(d_3)AcGGG-OtBu+Li]^+$ by the McLafferty rearrangement as described in chapter 1, scheme 1. In this case, the peptide *tert*-butyl ester was incubated and sprayed from a solution of D_2O and CH_3OD (thereby causing exchange of amide position hydrogen for deuterium in the solution phase). CID of



Scheme 2 Formation of ($b_2+17+Li$)⁺ from [AcGGG-OH+Li]⁺

$[\text{AcGGG-OH+Li}]^+$



Scheme 3 Formation of $(b_2-1+Li)^+$ from $[\text{AcGGG-OH+Li}]^+$

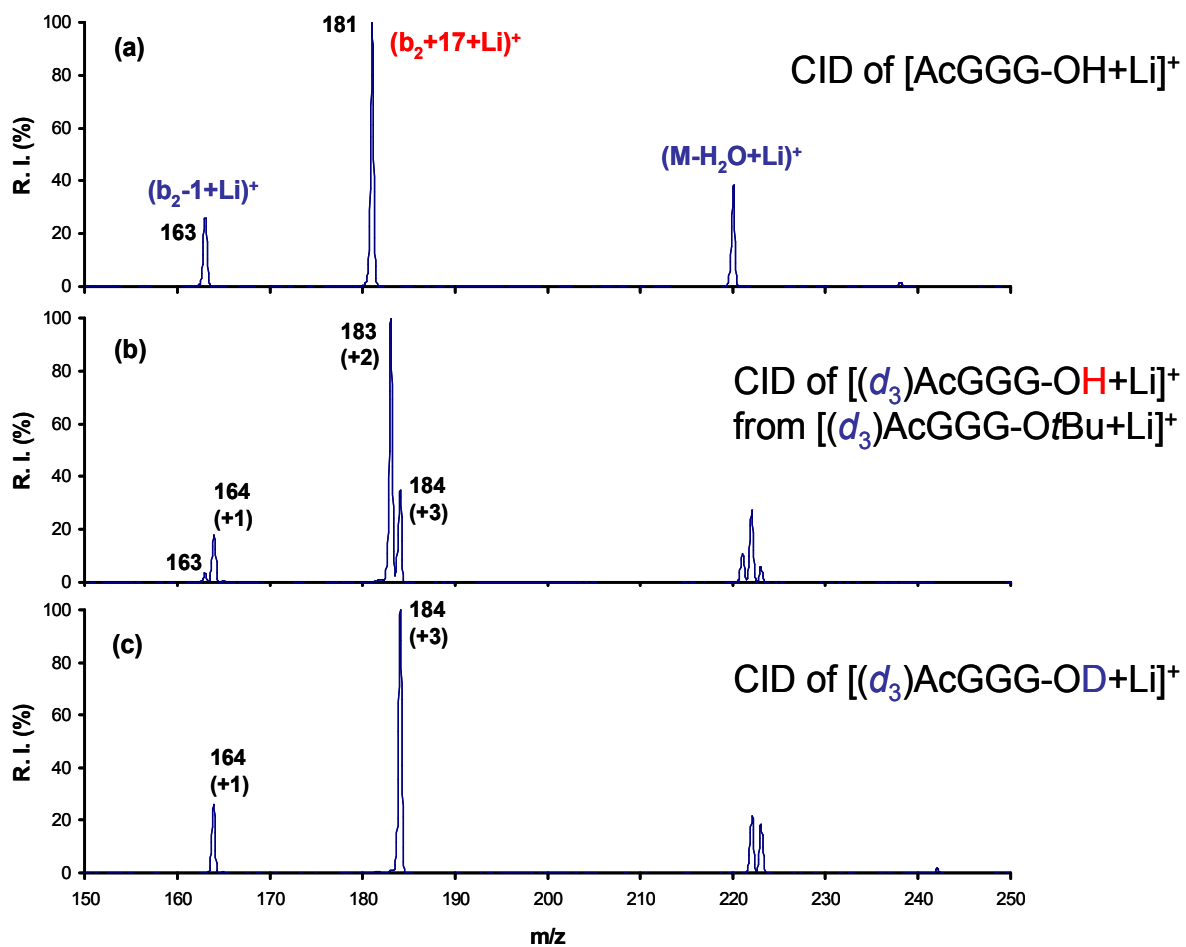


Figure 3.3 Three mass spectra generated by CID of three forms of AcGGG (a) CID of $[\text{AcGGG-OH}+\text{Li}]^+$. (b) CID of $[(d_3)\text{AcGGG-OH}+\text{Li}]^+$ formed from $[(d_3)\text{AcGGG-OtBu}+\text{Li}]^+$ by McLafferty rearrangement. (c) CID of $[(d_3)\text{AcGGG-OD}+\text{Li}]^+$ (the numbers in the parenthesis represent mass shifts) .

cationized, D-exchanged form of the peptide also induced the McLafferty-type rearrangement. In this case, however, the McLafferty-type rearrangement transferred H to the C-terminus of the peptide because the *tert*-butyl ester contained H rather than D. The transfer of H is therefore creation of the isotope label in-situ (chapter 1, scheme 1). In figure 3.3 (b), the $(b_2+17+Li)^+$ product ion generated is split into two isotopic peaks at m/z 183 and 184. The peak at m/z 183 was shifted by 2 Da relative to the non-labeled control (figure 3.3 (a)), consistent with the retention by the $(b_2+17+Li)^+$ product ion of 2 amide position D atoms and the H atom isotope label transferred during the CID reaction. The peak at m/z 184 was shifted instead by 3 Da, meaning that the 3 amide D atoms were retained by the product ion and that the isotope label (H atom) was eliminated as part of the imine neutral (see chapter 1, scheme 1). The peak at m/z 184 therefore represents isotope scrambling during the CID reaction. The CID (MS/MS) spectrum of $[(d_3)AcGGG-OD+Li]^+$ (i.e. fully deuterium exchanged) generated from the incubation of AcGGG in D_2O and CH_3OD is shown in figure 3.3 (c). In this case, all amide N positions and the C-terminal acid positions were labeled with D. No splitting of the $(b_2+17+Li)^+$ (m/z 184) and $(b_2-1+Li)^+$ (m/z 164) peaks was observed for the fully deuterium-exchanged peptide, demonstrating that the isotope peaks observed in figure 3.3 (b) do not originate from rapid gas-phase HDX with adventitious H_2O present within the ion trap mass spectrometer, or from the elimination of H from α -carbon positions.

For the *tert*-butyl ester, the McLafferty-type rearrangement involves transfer of γ -position H to the carbonyl O atom through a 6-member ring

intermediate [40, 41]. An important consideration when interpreting the peak splitting in figure 3.2 was whether the McLafferty-type rearrangement generated an ion population with isotope label (H atom) primarily at the C-terminal acid group, and proton migration/scrambling brought about solely by formation of the sequence ions in the subsequent CID stage. The scrambling could instead involve rapid, “global” exchange among all exchangeable sites directly following the McLafferty-type rearrangement but prior to the reactions to form product ions as induced in the subsequent CID stage. This point is particularly important to the potential use of the isotope label to investigate migration of the C-terminal acid H atom during the formation of the $(b_2+17+Li)^+$ ion (scheme 2). As noted earlier, the $(b_2-1+Li)^+$ species is generated through a mechanism that involves cyclization and intra-molecular attack from the N-terminal side of the cleavage site, and formation of this particular product ion should not involve the H atom at the C-terminal acid position. Any splitting of the $(b_2-1+Li)^+$ product into isotopic peaks could therefore be used as an indicator of the amount of intra-molecular proton migration occurring after the McLafferty-type rearrangement but prior to the CID stage used to create the $(b_2+17+Li)^+$ and $(b_2-1+Li)^+$ products. The major peak representing formation of $(b_2-1+Li)^+$ appeared at m/z 164 in figure 3.3 (c). The $(b_2-1+Li)^+$, if an oxazolinone type product, would retain a single amide position D atom, and the peak at m/z 164 is shifted by 1 Da relative to the unlabeled control (figure 3.3 (a)). Close inspection of the $(b_2-1+Li)^+$ species revealed a small peak at m/z 163 with an intensity of about 10% of the peak at m/z 164. The peak at m/z 163 has the same m/z value as $(b_2-1+Li)^+$ generated

from the unlabeled control peptide, and thus represents a situation in which the single amide position D atom was exchanged for the H atom isotope label. The low intensity of the peak at m/z 163 relative to m/z 164 suggests, however, that the amount of intra-molecular scrambling occurring prior to the CID stage used to generate the $(b_2+17+Li)^+$ and $(b_2-1+Li)^+$ is minor.

3.2 Influence of two important CID Parameters

There are two important parameters that can be varied during CID in the ion trap. The first one is the activation amplitude, which represents the amplitude of the R.F. voltage applied to the end cap electrodes of the ion trap to increase the ion kinetic energy and thus the energies of the collisions with the He bath gas. The activation amplitude setting on the LCQ is an arbitrary scale that represents a mass-normalized percentage of a maximum of 20 volts that can be applied to the end cap electrodes to affect collisional activation. For a given activation amplitude, the actual laboratory-frame of reference applied voltage applied to the electrodes is higher for high mass ions than for low mass ions. The second parameter is the activation time, which represents how long a precursor ion is stored in the ion trap and (resonantly) subjected to the collisional activation. As the activation amplitude and activation time might significantly affect the extent and rate of dissociation of the ions in the ion trap, thus influence the relative fragment ion abundances, it was important to investigate whether either setting significantly affect the peak splitting observed.

Figure 3.4 shows the influence of (a) activation amplitude and (b) activation time on the CID of Li⁺ cationized (*d*₃)AcGGG-OH generated from (*d*₃)AcGGG-*Ot*Bu. As is apparent in figure 3.4 (a), from the point where product ions are generated (at ~19% activation amplitude), no significant influence on the splitting due to the changes in activation amplitude was observed. As shown in figure 3.4 (b), the activation time also does not significantly influence the splitting observed.

3.3 Summary

The results here demonstrate that a McLafferty-type rearrangement of peptide C-terminal *tert*-butyl esters can be used to generate an isotope label in-situ. Intra-molecular scrambling of H and D during CID of peptide ions is exposed by the splitting of sequence ions into isotopic peaks.

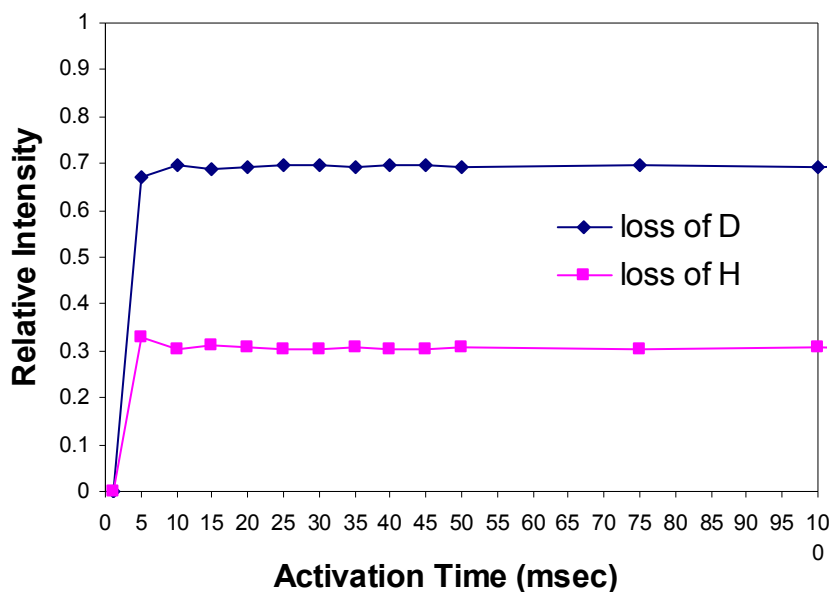
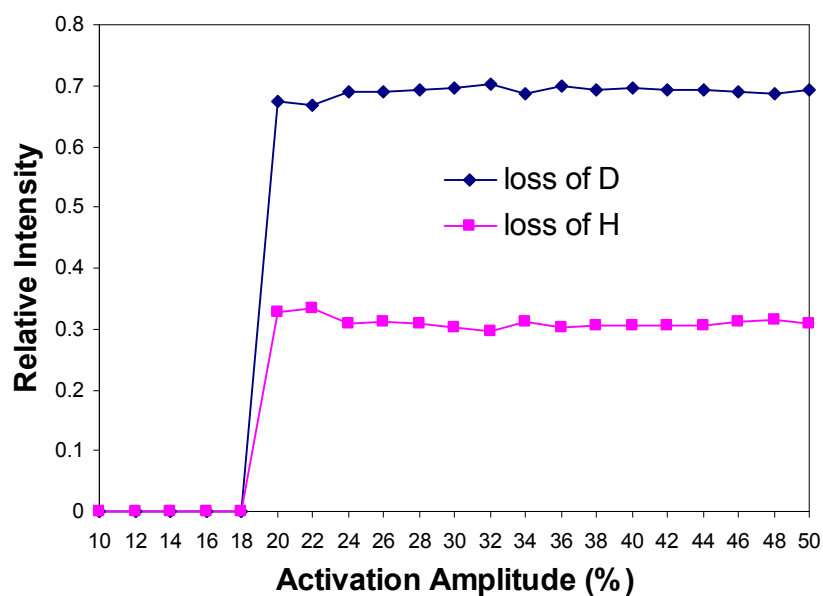


Figure 3.4 CID of Li⁺ cationized (*d*₃)AcGGA-OH generated from (*d*₃)AcGGA-O*t*Bu

CHAPTER 4

INFLUENCE OF POSITION AND NUMBER OF AMIDE EXCHANGEABLE SITES ON PEAK SPLITTING

4.1 Results from a Series of Sarcosine Substitution Peptides

Data in chapter 3 showed that a McLafferty-type rearrangement can be used to generate an isotope label, in-situ, at the C-terminus of a peptide ion. In these experiments, the goal was to determine the influence of the number and the position of possible amide-position exchange sites along the peptide backbone on the elimination of D or H during the formation of $(b_2+17+Li)^+$ product ion. Several analogues to AcGGG-OH were synthesized. In these peptides, sarcosine, or N-methyl glycine, was placed either at the C-terminus, in the middle position, or at the N-terminus of the peptides. Use of sarcosine eliminates the possibility for proton exchange to the substitution position, and thus allowed an investigation of the importance of the respective exchange positions to the splitting observed. Proline would also have eliminated an exchange. However, the cyclic structure of proline would likely disrupt any intra-molecular H/D exchange by inhibiting cyclization necessary for transfer from one amide position to another. For this study, the goal was to eliminate potential sites of proton transfer without disrupting potential cyclization.

As shown in figure 4.1 for $(d_3)AcGGG-OH$ (again, the subscript refers to the number of amide position D atoms), the key intermediate to formation of $(b_2+17+Li)^+$ contains four possible exchangeable sites (three are the amide N

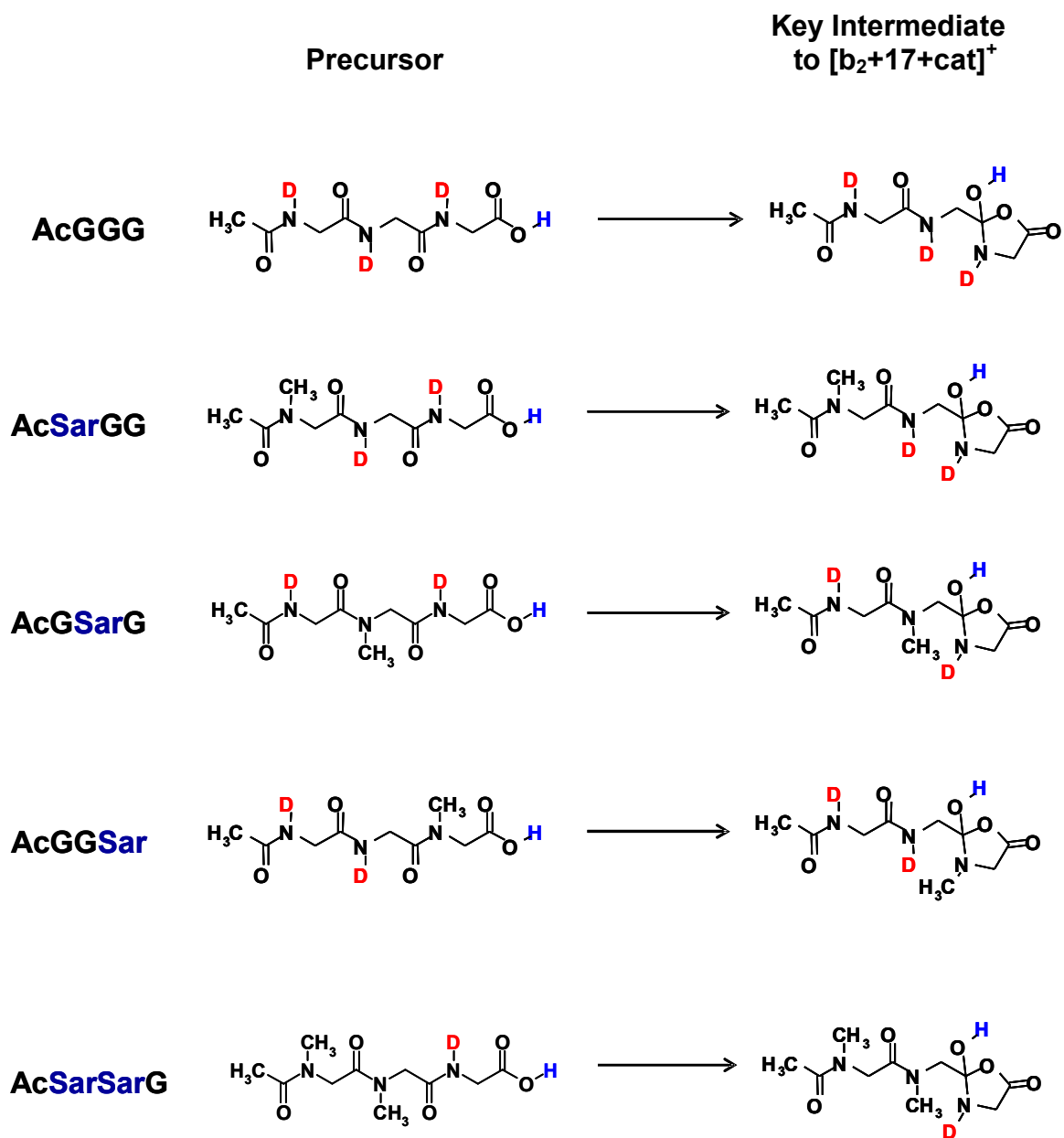


Figure 4.1 Precursor species, potential intermediates to $[b_2+17+cat]^+$ of peptides AcGGG, AcSarGG, AcGSarG, AcGGSar, AcSarSarG.

atoms and one is the C-terminal –OH group, as shown in chapter 1 scheme 1). For each of the peptides containing one sarcosine residue, one amide exchange position was eliminated, leaving two amide and one acid position as possible exchange sites. For (d_2)AcGGSar-OH, however, the amide group of the C-terminal amino acid contains a methyl group, thus eliminating the possibility for proton transfer to the N atom that eventually is part of the imine neutral product eliminated in formation of ($b_2+17+Li$)⁺. For (d_3)AcGGG-OH and the two other single sarcosine substituted peptides (d_2)AcGSarG-OH and (d_2)AcSarGG-OH, it is transfer of H to the first amide position, the one that leaves incorporated into the imine neutral, that leads to splitting.

Based on random probability, and assuming that full proton mobility and access to each exchange site is possible, for (d_3)AcGGG-OH, there is a one in four chance for the H atom to occupy an exchange site eliminated as a part of the imine neutral. According to this assumption, one would expect the probability for retention of the H atom transferred to the peptide by the McLafferty-type rearrangement to be about 75% and the elimination of D versus the elimination of H as part of the neutral imine product (i.e. loss of 58 Da relative to 57 Da) to be favored by a ratio of 3:1. For (d_2)AcGGSar-OH, the N atom eliminated in the reaction pathway bears a methyl group. There is no chance for H transfer to the imine portion. No splitting is expected to be observed because the exchange site on the neutral imine product is eliminated. For both (d_2)AcGSarG-OH and (d_2)AcSarGG-OH, one of the exchangeable sites retained by the product ion is blocked by a methyl group and there is a one in three chance for the proton to be

transferred to the C-terminal amide position. So the elimination of D in the imine versus elimination of H is predicted to decrease to a ratio of 2:1, again with the assumption of full proton mobility and access to each exchange site.

Figure 4.2 shows portions of the CID spectra, highlighting the m/z region containing the $(b_2+17+Li)^+$ peak, derived from Li^+ cationized $(d_3)AcGGG-OH$, $(d_2)AcGGSar-OH$, $(d_2)AcGSarG-OH$, $(d_2)AcSarGG-OH$ and $(d_1)AcSarSarG-OH$, respectively. In each case, the acid forms of the amide D exchanged peptides were generated in-situ by using the respective *tert*-butyl ester versions of the peptides and the McLafferty-type rearrangement as explained in chapter 3. As shown in figure 4.2, for the CID (MS^3) of $(d_3)AcGGG-OH$, the loss of D (elimination of 58 Da) relative to H (57 Da) in the dissociation reaction was favored by a ratio of $\sim 3:1$. This result suggests that the isotope label is free to exchange among any of the potential sites. As predicted, no splitting of the $(b_2+17+Li)^+$ peak was observed for $(d_2)AcGGSar-OH$, because the N atom of the C-terminal amide group was methylated, thus preventing exchange at that site. For $(d_1)AcSarSarG-OH$, there are only two adjacent exchange sites are present. The splitting ratio of the $(b_2+17+Li)^+$ peak in this case was $\sim 1.1:1$. This result demonstrates that the isotope label can occupy either of the two exchange sites in the peptides. Elimination of D relative to H in ratios of $\sim 2.4:1$ and $\sim 1.5:1$ were observed for $(d_2)AcSarGG-OH$ and $(d_2)AcGSarG-OH$, respectively. The ratio of 2.4:1 greater than 2:1 predicted for $(d_2)AcSarGG-OH$, which suggests that there is a barrier to transfer of isotope label to the N atom of the imine eliminated. The ratio of 1.5:1 for $(d_2)AcGSarG-OH$ is lower than the predicted 2:1 ratio. The low

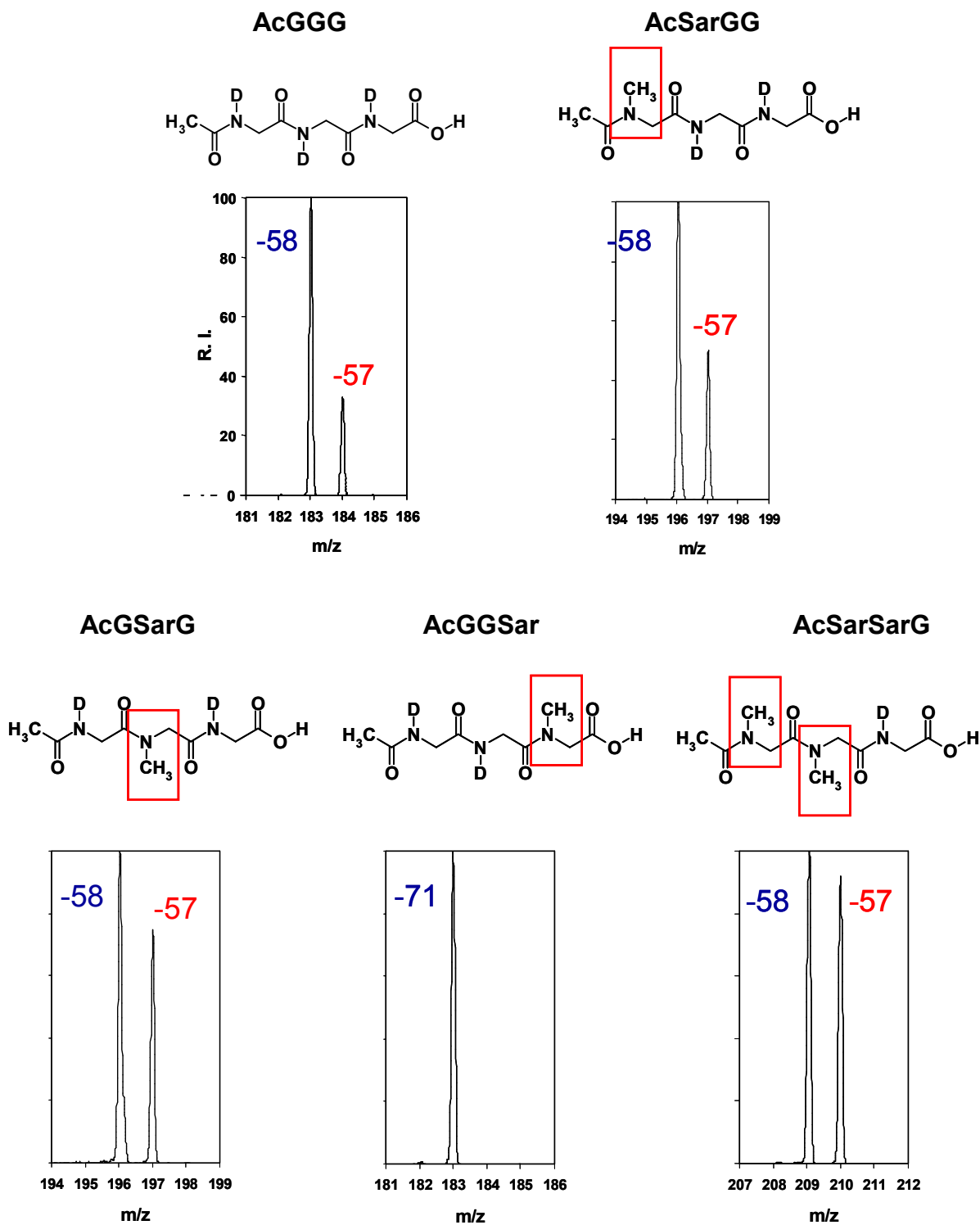


Figure 4.2 CID of $[(d_3)\text{AcGGG-OH+Li}]^+$, $[(d_2)\text{AcGGSar-OH+Li}]^+$, $[(d_2)\text{AcGSarG-OH+Li}]^+$, $[(d_2)\text{AcSarGG-OH+Li}]^+$, $[(d)\text{AcSarSarG-OH+Li}]^+$. In each case, species fragmented were derived by McLafferty rearrangement from *t*-butyl esters to generate isotope tracer.

ratio indicates that the H isotope label is more likely to be transferred to the imine neutral for this peptide. This can be explained by a decreased probability for migration of the isotope label to the amino terminal amide (the position furthest from the site when the label was generated) and the need to “hop” over a Sarcosine residue. This suggests that from migration of proton to N-terminal amide position is unfavorable. The result for (d_2)AcGSarG-OH is consistent with the proposed requirement for sequential tautomerism and cyclization steps to more “mobile” protons along the peptide CID reactions [42-44].

4.2 Summary

Taken together, the results from this suite of sarcosine substituted peptides suggest that the C-terminal acid and amide positions, and the amide position adjacent to the C-terminus, allow the exchange of the isotope label. Transfer to the amide position at the N-terminus, the position for which the distance from the site at which the isotope tracer was initially generated is the greatest, appears to be less favored.

CHAPTER 5

INFLUENCE OF AMINO ACIDS AND CATIONS ON INTRAMOLECULAR PROTON MIGRATION FROM THREE SERIES OF TRI-PEPTIDES

5.1 Introduction

The third goal of this study was to investigate the influence of different amino acids and cations on the amount of *intra*-molecular proton migration observed during formation of $[b_2+17+cat]^+$. For the isotope tracer method developed in this study to be generally applicable to determining the amount of *intra*-molecular proton migration, it is important to know the extent to which an amino acid at a given sequence might affect the potential for exchange at/to that site. In addition, peptide CID can involve different cationized forms of the molecule, so an investigation of the influence of cation on the amount of migration was also warranted. In the experiments described here, a survey was made of the influence of both amino acid and cation on the amount of isotopic peak splitting observed in the formation of $(b_2+17+Cat)^+$, using three series of synthetic acetylated tripeptide ester: AcSarGXOtBu, AcGSarXOtBu, AcSarSarXOtBu. The amino acid at position X was either glycine (G), alanine (A), valine (V), leucine (L) or phenylalanine (F). For generation of $[b_2+17+cat]^+$ from these peptides, the five member ring is composed of the amino acid X, and the different amino acid side groups thus lead to different substituted forms of the cyclic intermediates.

In chapter 4, the proof-of-principle experiments were conducted using Li^+ cationized, sarcosine-substituted peptides. In the experiments described in this chapter, peptides cationized by Na^+ and Ag^+ were compared to analogues cationized by Li^+ . Li and Na are both group I metal cations, with latter having a larger ionic radius and lower polarizing power than the former. In every case, CID of K^+ cationized peptides failed to produce product ions above the low-mass cut-off of the ion trap (ions above m/z 50 are not observed). It is likely that the main product ion from the K^+ cationized peptides is K^+ . CID of Rb^+ or Cs^+ produced the metal ions as the only product ions, consistent with the proposed explanation for a lack of product ions for the K^+ cationized versions. Ag^+ was chosen because it is a monovalent metal cation, and has been shown to produce somewhat different CID pathways than Li^+ and Na^+ , preferring in many cases to generate $(b_{n-1}+\text{Ag})^+$ ions over $(b_n+17+\text{Ag})^+$ species.

5.2 AcSarGXOtBu Series

Figure 5.1 shows the precursor ions and the potential intermediates to formation of $[b_2+17+\text{Cat}]^+$ for the series AcSarGXOtBu. Figure 5.2 shows the elimination of D versus the elimination of H as part of the neutral imine product in forming $[b_2+17+\text{Cat}]^+$ from peptides AcSarGXOtBu (X=G, A, V, L, F) cationized by (a) Li^+ (b) Na^+ (c) Ag^+ . The data in figure 5.2 are presented in bar graph form to show quantitatively the elimination of D versus H during formation of $[b_2+17+\text{Cat}]^+$. For Li^+ , a slight decrease in the amount of H eliminated, relative to D, was observed for the version of the peptide with G at the C-terminus. The

ratio D to H loss was similar for the peptides with A, V, L or F at the C-terminus. For the Na⁺ cationized peptides, within the error bars of the measurement, there remained a slight increase in the amount of H eliminated relative to D in the reaction pathway progressing from A to L, with a decrease again for the peptide with a C-terminal F residue. For the Ag⁺ cationized peptides, little difference was observed across the group of peptides.

5.3 AcGSarXOtBu Series

Figures 5.3 and 5.4 show structures, and the experimental results, respectively, obtained for the AcGSarXOtBu series of peptide cationized by the three different metal ions. For this series of peptides, a more pronounced influence of the amino acid and cation on the relative amounts of H and D eliminated in the reaction to form $[b_2+17+Cat]^+$ were observed. A sharp increase in the amount of H eliminated, relative to D, was observed progressing from G to F at the C-terminus. In addition, the change in ratio of H versus D eliminated increased most sharply between a peptide with C-terminal G or A when the Ag⁺ cationized versions of the peptides were examined. For both Na⁺ and Ag⁺, the amount of H eliminated decreased, relative to D, for the peptides with a C-terminal F residue. The trend observed with respect to the ratio of H and D loss is similar to trends in the influence of the C-terminal amino acid on the tendency to make the $[b_n+17+Cat]^+$ species [Anbalagan, JMS 2003]. The collision energies required to make the product ion decrease, following the trend G > A > V = L when these amino acids are at the C-terminus of a peptide. The reason why the amount of isotopic splitting should mirror the trend with respect to the

ease with which the $[b_n+17+Cat]^+$ product ion forms is not known, and merits an intensive computation study at a later date.

5.4 AcSarSarXOtBu Series

Figures 5.5 and 5.6 show structures and experimental results, respectively, obtained from the AcSarSarXOtBu series of peptides. In this series, the tendency to lose H relative to D increases progressing from G to F when the cation was Li^+ or Ag^+ . The change was less pronounced than for AcGSarXOtBu. For this series of peptides, the Na^+ cationized versions appear to be less influenced by the identity of the C-terminal amino acid.

5.5 Summary

The results obtained in this series of experiments indicate that the identity of the amino acid at a given position, and the choice of cation, can influence the amount of intra-molecular proton migration in peptide CID. The influence by the amino acid in particular does not follow a clear trend. At best, it is safe to say that the degree to which the isotope label was eliminated as part of the neutral product during formation of $[b_2+17+Cat]^+$ was lowest for peptides with C-terminal G, and increased as the C-terminal residue was changed to amino acids with larger α -carbon side groups such as A, V or L. The experiments show that, in general, the influence of the C-terminal amino acid was greatest for the peptides with a sarcosine residue in the middle position, that is, the peptides in which the isotope tracer would have to migrate to the N-terminal residue to reach the an

amide exchange site. As shown in Chapter 4, transfer to this position is unfavorable. The results obtained in the experiments described here might be clarified by a computational investigation of the tendency to form the $[b_2+17+Cat]^+$ ion from peptides with the respective C-terminal amino acids, as well as the relative proton affinities and gas-phase basicities of the N-atom within the cyclic intermediate relative to the amide and $-OH$ positions.

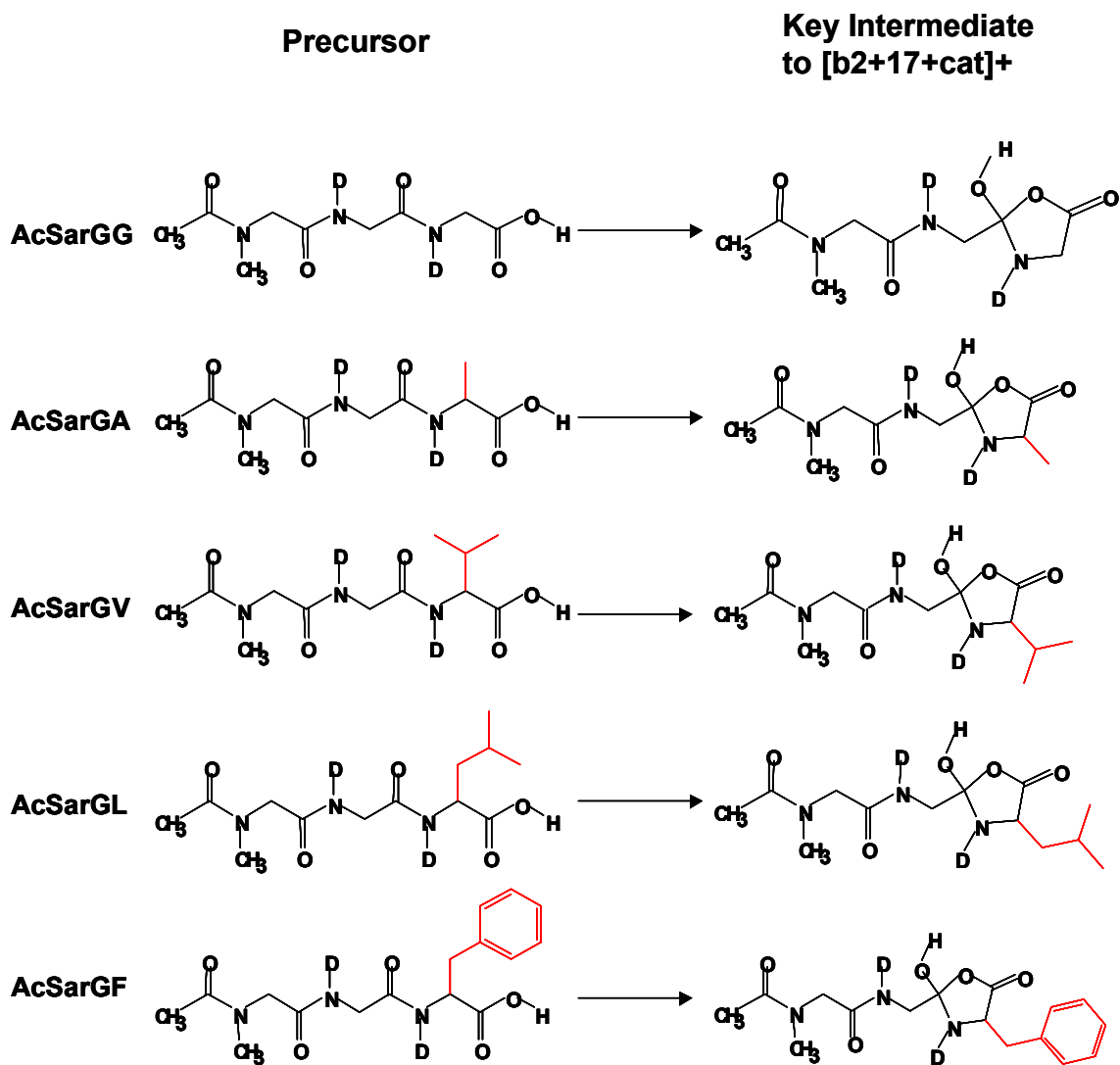


Figure 5.1 Precursor species, potential intermediates to [b2+17+cat]+ of peptides AcSarGX (X=G, A, V, L, F)

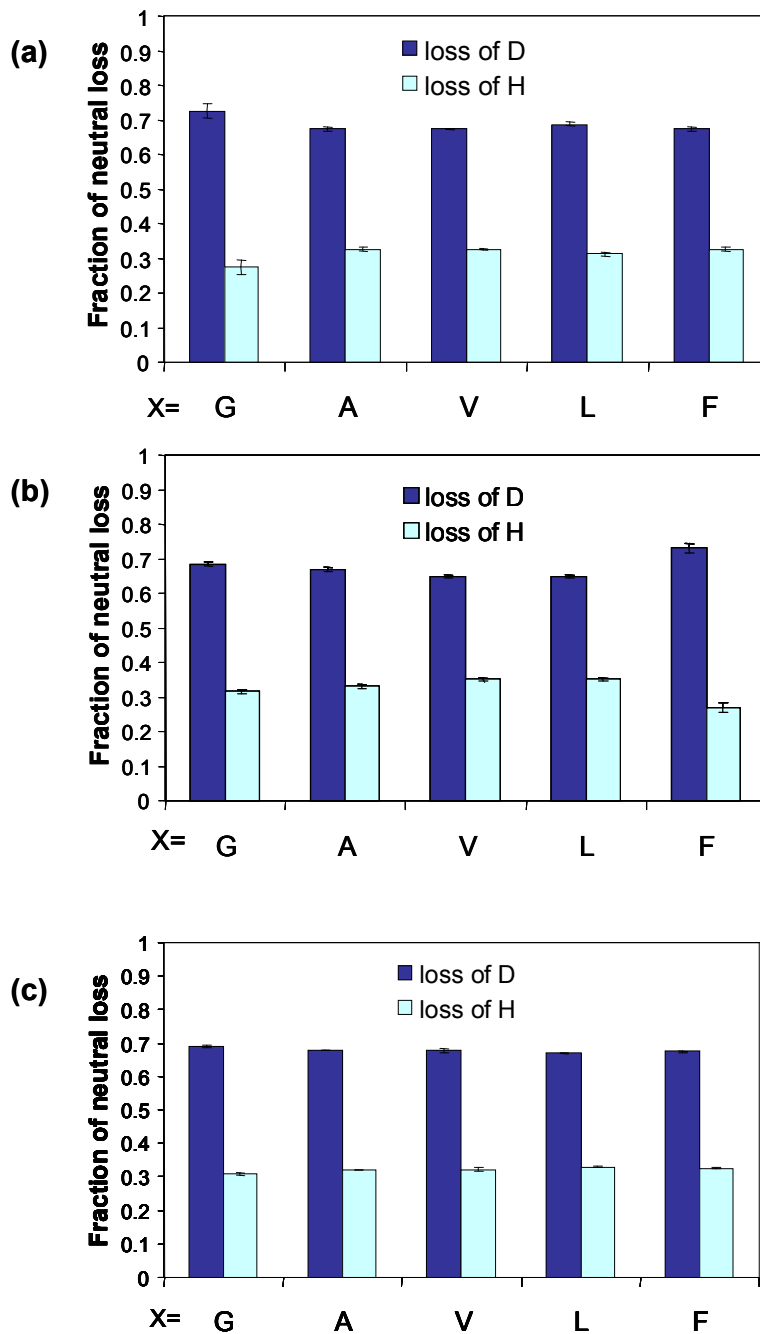


Figure 5.2 Elimination of D versus the elimination of H as part of the neutral imine product in forming $[b2+17+cat]^+$ of peptides AcSarGX (X=G, A, V, L, F) with different cations. (a) Li⁺ (b) Na⁺ (c) Ag⁺ (the error bars represents the standard deviation based on three trials)

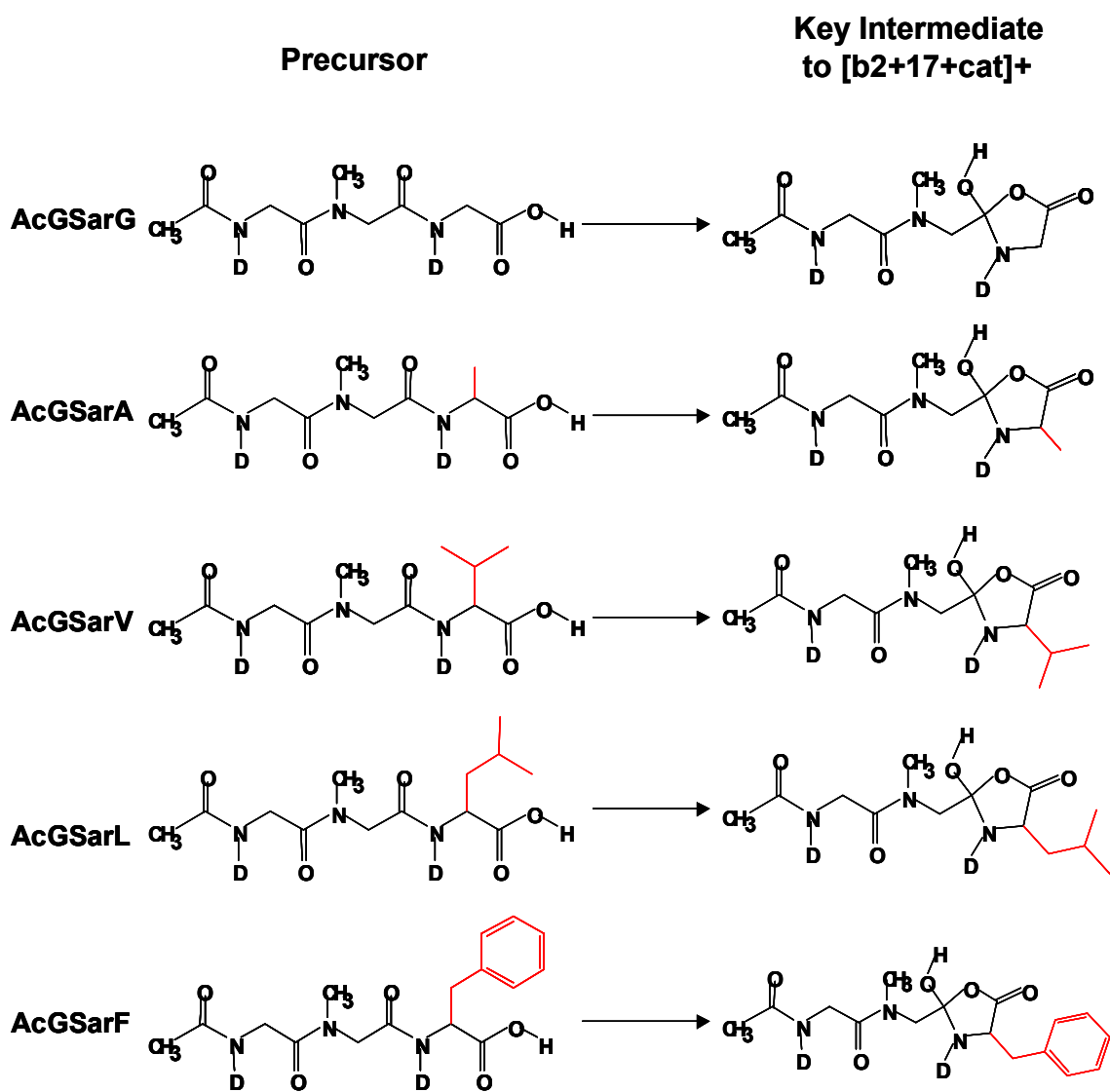


Figure 5.3 Precursor species, potential intermediates to [b2+17+cat]+ of peptides AcGSarX (X=G, A, V, L, F)

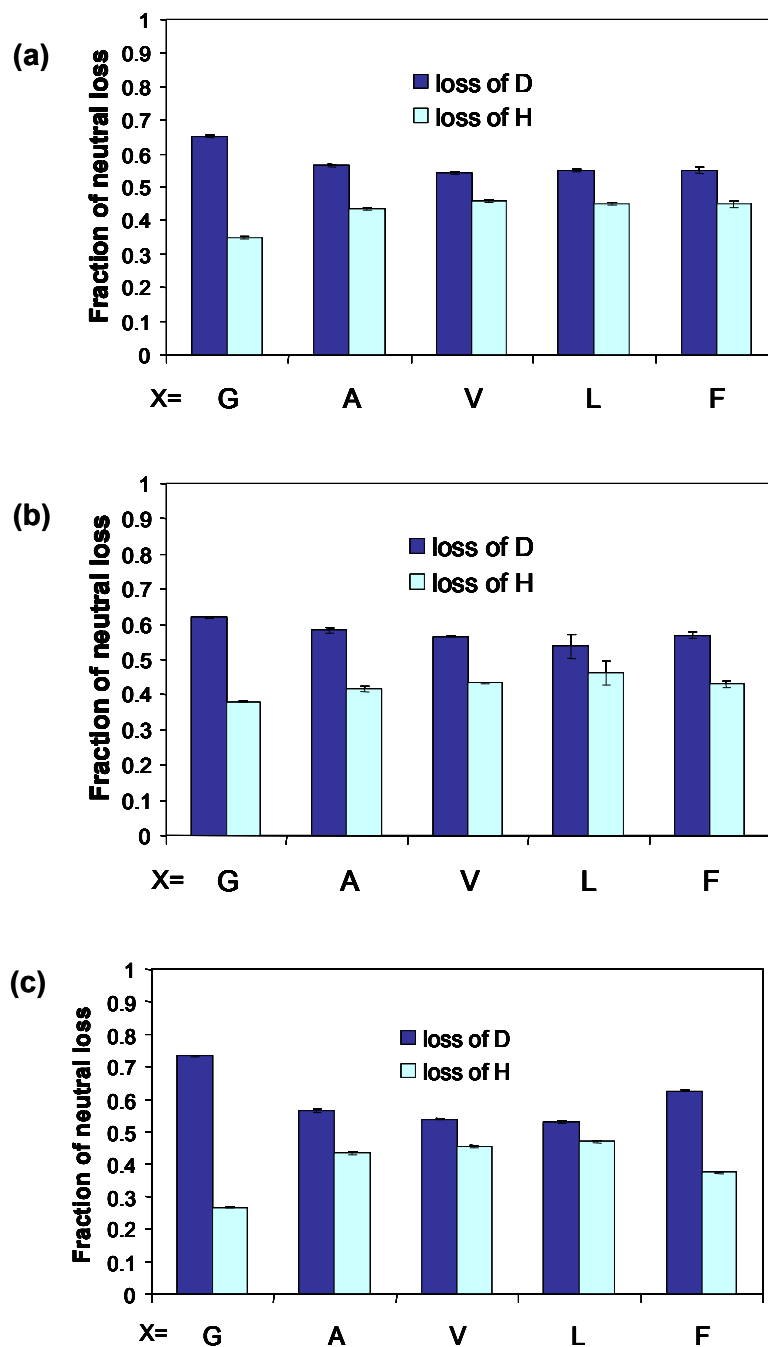


Figure 5.4 Elimination of D versus the elimination of H as part of the neutral imine product in forming $[b2+17+cat]^+$ of peptides AcGSarX (X=G, A, V, L, F) with different cations. (a) Li⁺ (b) Na⁺ (c) Ag⁺ (the error bars represents the standard deviation based on three trials)

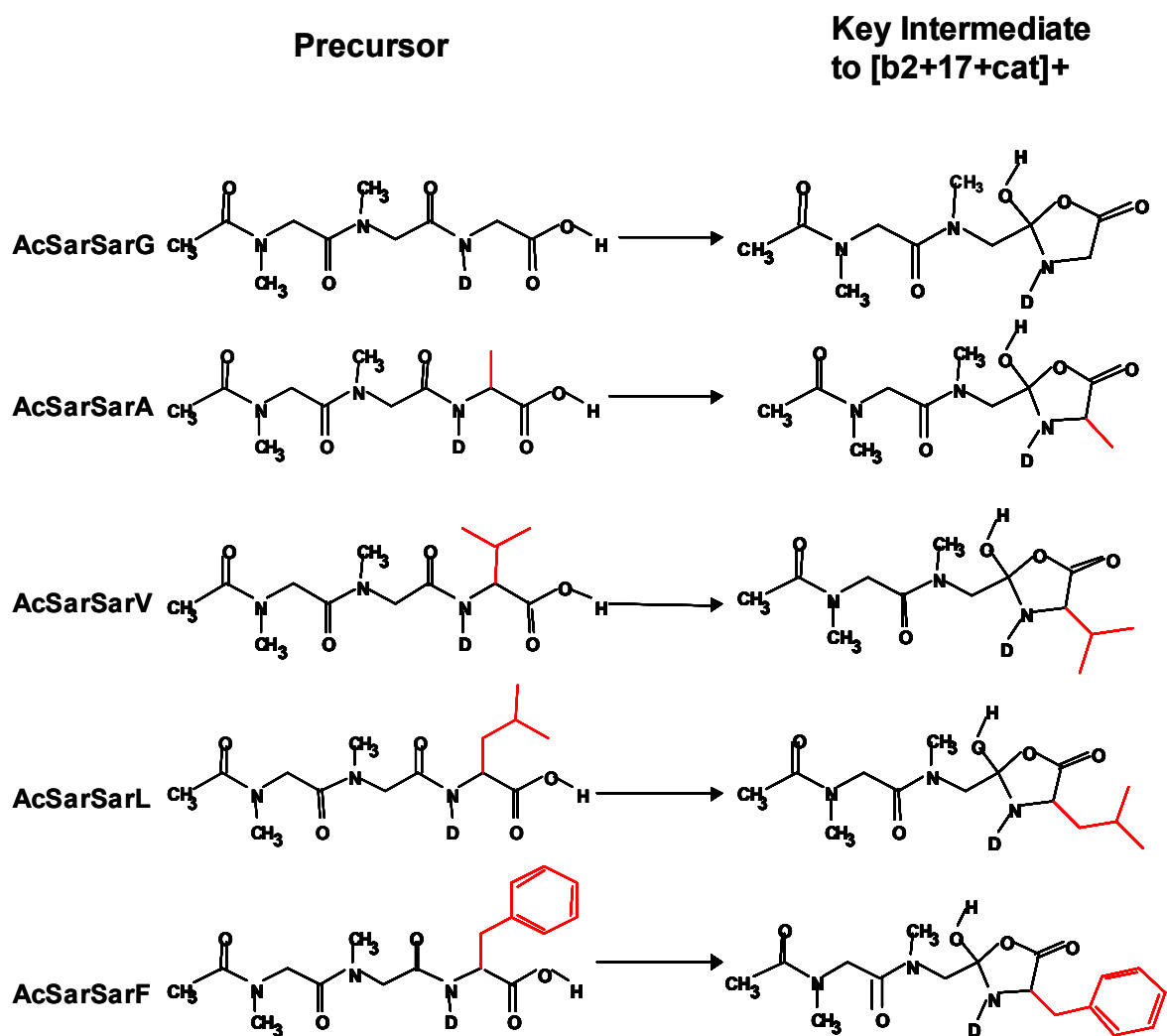


Figure 5.5 Precursor species, potential intermediates to [b2+17+cat]⁺ of peptides AcSarSarX (X=G, A, V, L, F)

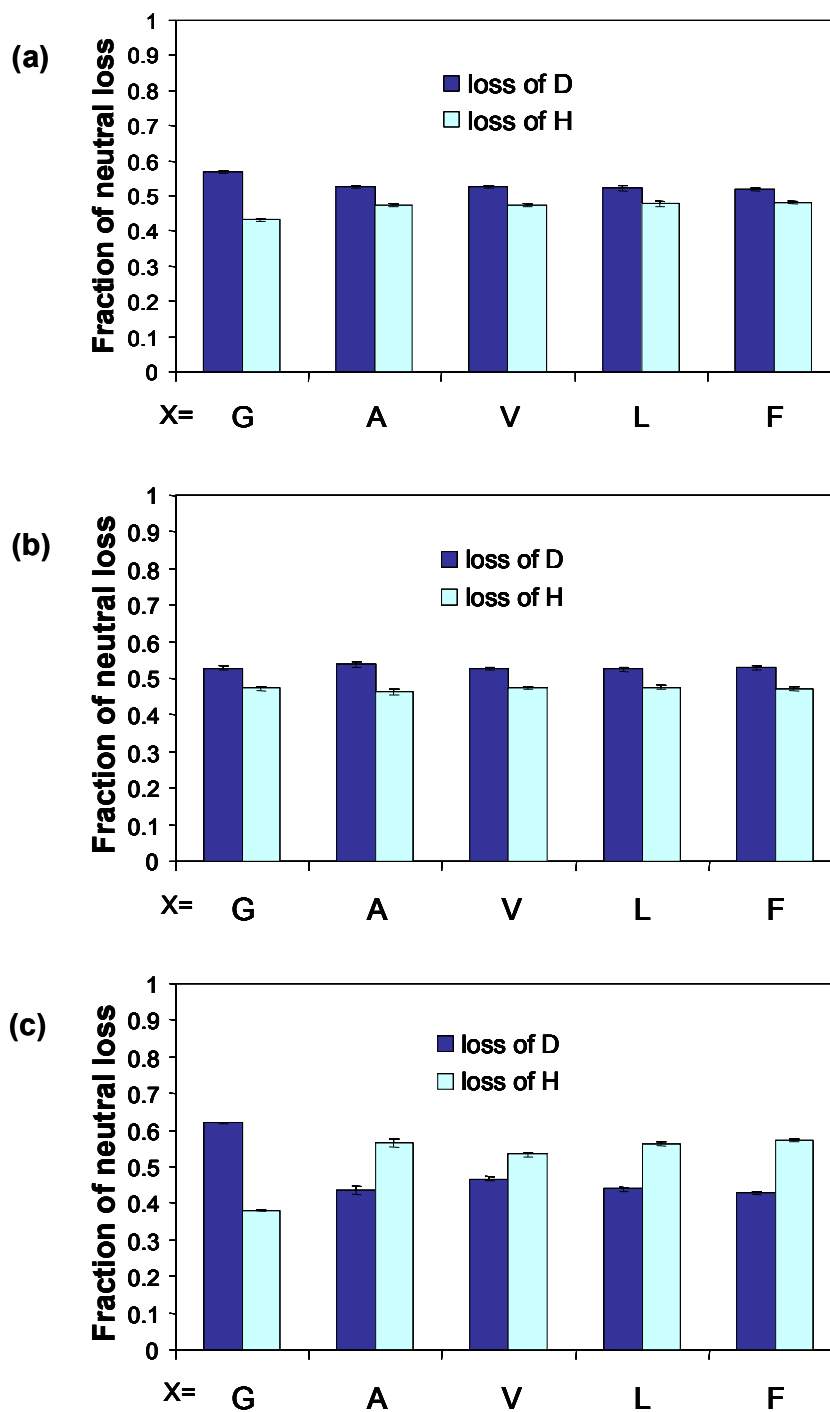


Figure 5.6 Elimination of D versus the elimination of H as part of the neutral imine product in forming [b2+17+cat]⁺ of peptides AcSarSarX (X=G, A, V, L, F) with different cations. (a) Li⁺ (b) Na⁺ (c) Ag⁺ (the error bars represents the standard deviation based on three trials)

CHAPTER 6

CONCLUSIONS AND FUTURE WORK

The McLafferty-type rearrangement can be used to generate an isotope label/tracer at the C-terminus of a peptide. The intra-molecular migration and/or scrambling of the label can then be traced through fragmentation reactions induced by collisional activation. The experiments described in Chapter 3 strongly suggest that the isotope label is generated at the C-terminal acid group after the McLafferty rearrangement. The label can then participate in the gas-phase reaction to produce the $[b_2+17+Cat]^+$ ion from an acetylated tripeptide. Because one amide-position hydrogen atom is eliminated in the reaction, production of this fragment can be used to measure the amount of scrambling of protons in the CID. A suite of tripeptides containing glycine and one or two sarcosine residues were synthesized and used to study the extent to which the isotope label is transferred or scrambled among possible amide exchange sites. Results from the series of sarcosine substitution peptides show that C-terminal acid and amide positions, and the amide position adjacent to the C-terminus, allow the exchange of the isotope label. From a comparison of our AcSarGXOH and AcGSarXOH data we can conclude that proton migration is not limited to the most adjacent amide position. However, exchange to the N-terminal amide position was found to be particularly most unfavorable, which is consistent with the proposal that proton migration along a peptide backbone requires multiple

cyclization and proton transfer steps. The greater the number of cyclization and proton transfer steps, the lower the probability for proton migration.

The experimental results from CID of three series of synthetic acetylated tri-peptide esters AcSarGXOtBu, AcGSarXOtBu, AcSarSarXOtBu (where X= G, A, V, L, F) together with three different cations Li^+ , Na^+ , Ag^+ reveal that cations and amino acids have an influence on the proton migration. In general, the trend with respect to the elimination of the H atom isotope label in the reaction to produce the $[\text{b}_2+17+\text{Cat}]^+$ species from these peptides is that such an event is least likely when the C-terminal amino acid is glycine, but becomes more favorable when the C-terminal amino acid is an amino acid such as alanine, valine or leucine. This observation is consistent with the observed influence of the C-terminal amino acid on the tendency to form the $[\text{b}_n+17+\text{Cat}]^+$ product ion in general. The exact cause for the influences of amino acid and cation on the amount of H atom scrambling in the reaction requires a detailed computational chemistry investigation. The results presented here demonstrate that significant scrambling does occur within the suite of small peptides. Future work will involve the examination of larger peptides and peptides which feature the site-specific incorporation of amino acids that block the migration of “mobile” protons by influencing the size of key reaction intermediates or by blocking cyclization altogether, such as aminocaproic acid and *p*-amino benzoic acid. Just as taking away exchange sites by incorporation of sarcosine significantly influenced the amount of isotope splitting for the $[\text{b}_n+17+\text{Cat}]^+$ product, so too should the

suppression of cyclization, and therefore transfer of protons along the peptide backbone, have an effect.

In addition, the ability to produce the isotope label at the N-terminus of the peptide will be examined using the CID of peptides containing an N-terminal *tert*-butoxycarbonyl (Boc) protecting group. CID of peptides containing a Boc group causes the elimination of both isobutene and CO₂ to generate a free amino group. These two reactions could be exploited to generate an N-terminal H label in fashion similar to the McLafferty rearrangement used in these experiments.

The CID of protonated peptides was not investigated using the group of acetylated tripeptides because the lack of a basic group on the peptide made protonation difficult. The use of larger peptides, or peptides without N-terminal acetyl groups, would likely permit the study of proton migration in protonated peptides. The study of protonated peptides would be particularly important, because the major fragments ion generated from these species are the b_n^+ and y_n^+ products, the formation of which occurs through mechanisms significantly different from that operating in the formation of $[b_2+17+Cat]^+$ from the metal cationized peptides. Most importantly, the formation of b_n and y_n ions from protonated peptides does not include or involve the isotope label that would be generated by the McLafferty rearrangement, and would thus be another excellent probe for intramolecular proton scrambling. It is important to note also that the CID of Ag⁺ cationized peptides generates fragment ions that are common to both protonated and Li⁺ or Na⁺ cationized peptides. These experiments would

contribute greatly to our understanding of the migration of protons in CID reactions.

LIST OF REFERENCES

1. Lee, S. W.; Lee, H. N.; Kim, H. S.; Beauchamp, J. L. *J. Am. Chem. Soc.* 1998; 120: 5800.
2. Engen, J. R.; Smith, D. L. *Analytical Chemistry*. 2001; 73(9): 256A.
3. Emeric, G. T.; Kozlowski, J.; Zhang, Z.; Smith, D. L. *Anal. Chem.* 1992; 64: 2456.
4. Jurchen, J. C.; Cooper, R. E.; Williams, E. R. *J. Am. Soc. Mass Spectrom.* 2003; 14: 1477.
5. Kim, M. Y.; Maier, C. S.; Reed, D. J.; Deinzer, M. L. *J. Am. Chem. Soc.* 2001; 123: 9860.
6. Anderegg, R. J.; Wagner, D. S.; Stevenson, C. L. and Borchardt, R. T. *J. Am. Soc. Mass Spectrom.* 1994; 5: 425.
7. Katta, V.; Chait, B. T.; *Rapid Commun. Mass Spectrom.* 1991, 5, 214-217.
8. Akashi, S.; Naito, Y. and Takio, K. *Anal. Chem.* 1999; 71: 4974.
9. Buijs, J.; Hagman, C.; Hakansson, K.; Hinnerk Richter, J.; Hakansson, P. and Oscarsson, S. *J. Am. Soc. Mass Spectrom.* 2001; 12: 410
10. Demmers, J. A. A.; Rijkers, D. T. S.; Haverkamp, J; Killian, J. A. and Heck, A. J. R. *J. Am. Chem. Soc.* 2002; 124: 11191.
11. Deng, Y.; Pan, H. and Smith, D. L. *J. Am. Chem. Soc.* 1999; 121: 1996.
12. Eyles, S. J.; Speir, J. P.; Kruppa, G.H.; Gierasch, L. M. and Kaltashov, I. A. *J. Am. Chem. Soc.* 2000; 122: 495.
13. Heck, A. J. R.; Jorgensen, T. J. D.; O'Sullivan, M.; Raumer, M. V. and Derrick, P. J. *J. Am. Soc. Mass Spectrom.* 1998; 9: 1255.
14. McLafferty, F. W.; Guan Z.; Haupts, U.; Wood, T. D.; and Kelleher, N. L. *J. Am. Chem. Soc.* 1998; 120: 4732.
15. Cassady, C. J. *J. Am. Soc. Mass Spectrom.* 1998, 9, 716-23.
16. Kaltashov, I. A.; Doroshenko, V. M.; Cotter, R. J. *Proteins*. 1997, 28, 53.
17. Harrison, A. G. and Yalcin, T. *Int. J. Mass Spectrom.* 1995; 165: 339.
18. Johnson, R. S.; Krylov, D. and Walsh, K.A. *J. Mass Spectrom.* 1995; 30: 386.
19. Anbalagan, V.; Patel, J. N.; Niyakorn, G. and Van Stipdonk, M. J. *Rapid Comm. Mass Spectrom.* 2003; 17: 291.

20. Anbalagan, V.; Perera, B. A.; Silva, A. T. M.; Gallardo, A. L.; Barber, M.; Barr, J. M.; Tekarli, S. M.; Talaty, E. R.; Van Stipdonk, M. J. *J. Mass Spectrom.* 2002; 37: 910.
21. Cooks, R. G., Beynon, J. H., Caprioli, R. M. *et al.*, *Metastable ions*. Elsevier, Amsterdam, 1973.
22. McLafferty, F. W. *Tandem Mass Spectrometry*. Wiley, New York, 1983.
23. Busch, K. L., Glish, G. L., and McLuckey, S. A. *Mass Spectrometry/ Mass Spectrometry: techniques and Applications of Tandem Mass Spectrometry*, VCH, New York, 1988.
24. Jennings, K. R. *Int. J. Mass Spectrom. Ion Phys.* 1968; 1: 227.
25. Yost R. A. and Enke, C. G. *J. Am. Chem. Soc.* 1978; 100: 2274.
26. Chapman, S. *Physical Review*, 1937; 10:184.
27. Dole, M.; Mack, L. L.; Hines, R. L. *Journal of Chemical Physics*.1968; 49: 2240.
28. Mack, L. L.; Kralik, P.; Rheude, A.; Dole, M. *Journal of Chemical Physics*. 1970; 52: 4977.
29. Yamashita, M.; Fenn, J. B. *Journal of Physical Chemistry*, 1984; 88: 4451.
30. Fenn, J. B.; Mann, M.; Meng, C. K.; Wong, S. F.; Whitehouse, C. M. *Science*, 1989; 246: 64.
31. Paul W.; Steinwedel H. S. *US Patent*, 1960, 2 939 952.
32. Stafford, G. C.; Kelley, P. E.; Syka, J. E. P.; Reynolds, W. E. and Todd, J. F. *J. Int. J. Mass Spectrom. Ion Processes*, 1984; 60: 85.
33. Grese, R. P.; Cerny, R. L.; Gross, M. L. *J. Am. Chem. Soc.* 1989; 111: 2835.
34. Teesch, L. M.; Orlando, R. C.; Adams, J. *J. Am. Chem. Soc.* 1991; 113: 3668.
35. Chu, I. K.; Shoeib, T.; Guo, X.; Rodriguez, C. F.; Lau, T. C.; Hopkinson, A. C.; Siu, K. W. M. *J. Am. Soc. Mass Spectrom.* 2001; 12:163.
36. Renner, D.; Spiteller, G. *Bio. Environ. Mass Spectrom.* 1988; 15:75.
37. Yalcin, T.; Khouw, C.; Csizmadia, I. G.; Peterson, M. R.; Harrison, A. G. *J. Am. Soc. Mass Spectrom.* 1995; 6: 1164.

38. Yalcin, T.; Csizmadia, I. G.; Peterson, M. R.; Harrison, A. G. *J. Am. Soc. Mass Spectrom.* 1996; 7: 233.
39. Schlosser, A.; Lehmann, W. D. *J. Mass Spectrom.* 2000; 35: 1382.
40. McLafferty, F. W. *Anal. Chem.* 1956; 28: 306.
41. Gilpin, J. A., McLafferty, F. W. *Anal. Chem.* 1957; 29: 990.
42. Csonka, I. P.; Paizs, B.; Lendvay, G. Suhai, S. *Rapid Comm. Mass Spectrom.* 2001, 15: 1457.
43. Paizs, B. Csonka, I. P.; Lendvay, G. Suhai, S. *Rapid Comm. Mass Spectrom.* 2001, 15: 637.
44. Rodriguez, C. F.; Cunje, A.; Shoeib, T.; Chu, I. K.; Hopkinson, A. C.; Siu, K. W. M. *J. Am. Chem. Soc.* 2001, 123: 3006.